Journal of the
OPTICAL SOCIETY *of* AMERICA

VOLUME 31 AUGUST, 1941 NUMBER 8

Comparison of Graininess and Speeds of Different Types of Photographic Films

C. E. BARTHEL, JR.
Department of Physics, Iowa State College, Ames, Iowa
(Received December 2, 1940)

In this investigation the graininess and speed of the more popular commercial films developed in typical fine-grain developers were determined quantitatively. It was found that the differences in graininess produced by the developers were small in comparison with the inherent differences among the various films. Certain fine-grain developers were effective in reducing the graininess of fast, coarse-grain emulsions, but only at the sacrifice of effective emulsion speed. These developers, however, were only slightly effective in reducing the graininess of slow, fine-grain emulsions, small differences in density or contrast completely obscuring the effects of the developers.

I. INTRODUCTION

THE amateur and professional photographers of today have at their disposal numerous types of photographic films of widely different characteristics. The serious workers may obtain information concerning the more important characteristics of these films from their manufacturers, but often the data supplied are insufficient and, in some cases, inaccurate.

The principal photographic properties of any emulsion may be listed as follows: (1) speed or sensitivity; (2) grain size and granularity; (3) color sensitivity; (4) contrast; and (5) latitude. These properties vary tremendously for different films, and all except the color sensitivity vary considerably for a given film in different developers and under different conditions of processing.

Innumerable developers are available for photographic use, the manufacturers claiming phenomenal properties for their products. These manufacturers, however, provide little or no specific data on the behavior of typical films in their developers, and if data are supplied, they are often partial or incorrect.

The investigation under consideration was undertaken to provide for the serious photographer impartial comparative data on the graininess and speed of the more popular commercial films developed in typical developers under uniform processing conditions.

II. REVIEW OF LITERATURE

A. Graininess and granularity

1. *Grain size and graininess.*—The individual silver grains of a photographic deposit vary in size for different emulsions, their average areas varying from approximately 0.1×10^{-8} cm² for slow positive emulsions to 1×10^{-8} cm² for fast negative emulsions. Consequently, individual silver grains are observable only at very high magnification. However, even at relatively low magnification, enlarged positive prints exhibit a definite inhomogeneity due to the grouping of several grains into clumps or to the superposition

BOSTON UNIVERSITY
COLLEGE OF LIBERAL ARTS
LIBRARY

of several grains in different layers of the emulsion. This inhomogeneity is commonly referred to as graininess* to distinguish it from the effect produced by the resolution of individual grains.

Many conflicting investigations on grain size and the development process were made in the early days of photography by such pioneers as A. and L. Lumière and A. Seyewetz,[18] R. J. Wallace,[28] S. E. Sheppard and C. E. K. Mees,[25] and others. It was not until 1917, however, that M. B. Hodgson,[9] definitely differentiated between grain size and graininess in the photographic image. Since the photographer is more concerned with the graininess of the silver deposit than with the size of the individual grain, this differentiation aroused a new interest in fine-grain photography, resulting in many investigations of theoretical and practical value. These investigations have shown that the graininess of the photographic image is a function of the size and the distribution of individual silver grains, and E. W. H. Selwyn[24] has even published a mathematical theory of graininess in which the direct relationship between graininess and grain size is given. Other mathematical theories based upon the average transparency fluctuation of a uniformly exposed area have been developed, the one proposed by A. Dember, A. Goetz, and W. O. Gould[4] arousing particular interest.

2. *The measurement of graininess.*—Many investigators have obtained important qualitative information on the graininess of certain photographic materials by visually comparing enlargements made from these materials and magnified to the same degree.

A procedure for measuring graininess quantitatively is to make a series of carefully prepared enlargements from a given material and to use as an index of measurement the magnification at which the inhomogeneity of the material first becomes apparent.

An equivalent method that eliminated the preparation of a series of enlargements for each material was developed by L. A. Jones and N. Deisch[12] in 1920. They devised an apparatus for viewing a magnified image at different distances and assumed that the graininess of a given material is proportional to the distance at which the appearance of inhomogeneity is just perceptible under definite viewing conditions. Two years later A. C. Hardy and L. A. Jones[7] suggested an improved technique capable of remarkable precision in graininess measurements, and in 1936 E. M. Lowry[17] described another apparatus which permitted varying magnifications at a constant viewing distance. A related method utilizing a comparison microscope for balancing the graininess of a sample material against that of an arbitrary standard under constant viewing conditions has been discussed by O. E. Conklin.[2] The relative magnification of the two images was used as a measure of graininess.

To eliminate discrepancies caused by differences in visual acuity of the observers and changes in acuity of a given observer from moment to moment, Jones and Deisch and subsequent workers required that the blending distance for the material under consideration be compared with that of an arbitrary standard, usually a printer's half-tone screen.

Objective methods for measuring granularity have been developed by S. D. Threadgold,[26] A. van Kreveld,[15] V. Ronchi,[22] Goetz and Gould,[6] and others; but since graininess is a subjective impression on the retina of the eye, these methods have failed to supplant the subjective methods listed above.

3. *Factors affecting graininess and granularity.*—Shortly after the development of the devices permitting accurate quantitative measurements on graininess, a tremendous amount of research on the control of graininess was excited by the lively interest of workers in the motion picture industry.

A theoretical consideration of the size and distribution of opaque clumps of silver grains shows that maximum graininess should occur at a transmission of 0.5 or an optical density of 0.3, the density at which the total area occupied by the grains is just equal to the total area of the spaces between grains. Hardy and Jones[7] and other workers found that the density giving maximum graininess depends upon several factors, and their results differ from the theoretical

* In this paper granularity refers to certain physical characteristics of the developed silver image, while graininess refers to the psychophysical evaluation of the inhomogeneities of the silver image.

value of 0.3, but it must be remembered that that value applies only for completely opaque silver grains. A. van Kreveld and J. C. Scheffer,[16] F. L. English,[5] George Higgins,[8] and other investigators have shown that graininess, or granularity, increases with the degree of development or gamma. This important factor was neglected in early, and in many recent, investigations on graininess control, rendering the results worthless.

The influence of processing conditions—such as temperature variation between solutions, temperature of washing, and drying conditions—upon graininess have been considered, but few conclusive data have been obtained. A. Marriage[20] reported that sudden changes in temperature and widely varying drying conditions have no observable effect, and J. I. Crabtree[3] has suggested that an incipient reticulation often observed in enlargements may be mistaken for graininess. The manufacturers and users of photographic materials, however, hesitate to accept these results as conclusive.

4. *Fine-grain development.*—The increasing popularity of the miniature camera has resulted in the preparation of numerous so-called fine-grain developers involving every imaginable type of developing agent.

Van Kreveld and Scheffer[16] reported that certain fine-grain developers are effective in reducing the granularity of fast, coarse-grain emulsions but are practically ineffective for slow, fine-grain emulsions. G. Schwarz,[23] on the other hand, found that fine-grain developers reduce the graininess of slow, fine-grain emulsions to a certain extent, but in most cases the differences in graininess produced by standard and fine-grain developers are negligible. In a thorough investigation of many developers Higgins[8] reported that certain developers are effective in reducing the graininess of fast, coarse-grain emulsions and are slightly effective for slow, fine-grain emulsions, but only at the expense of effective emulsion speed. He concluded that manufacture is more important in the control of graininess than the method of development employed.

B. Speed

Many methods of specifying the speed or sensitivity of a photographic emulsion have been devised, and the details of the more important methods, their advantages and disadvantages, have been described by L. A. Jones,[11] C. B. Neblette,[21] J. E. Mack and M. J. Martin,[19] and other writers. Photographers have recently become enthusiastic over the minimum useful gradient method, since the quality of a reproduction depends upon the gradient characteristics of the photographic material rather than upon the density, and since this method considers the useful region of underexposure as well as the linear portion of the characteristic curve in expressing speed.

In 1935, L. A. Jones and M. E. Russell[14] listed the advantages of the method and suggested the use of that exposure at which the gradient of the characteristic curve is some fraction of the maximum gradient to which the material is developed as a minimum useful exposure and an index for speed measurement. Since that time, however, L. A. Jones[10] and L. A. Jones and C. N. Nelson[13] have accumulated a mass of statistical data which proves conclusively that the exposure value at which the gradient of the characteristic curve is a definite fraction of the average gradient of a specified part of the curve is the most practical index, and Clifton Tuttle[27] has described procedures and instruments for the determination of emulsion speeds by this method.

In spite of the advantages of the method and the enthusiasm of the photographers, very little practical data on the sensitivity of photographic emulsions as determined by the minimum useful gradient method have appeared in the literature. At the present time, however, it is generally believed that this method will ultimately supplant other methods of speed specification.

III. Experimental

A. Statement of problem

In this investigation, the relative graininess and speed of eleven of the more popular commercial 35-millimeter miniature camera films developed in four typical fine-grain developers were determined. The films selected were Finopan, Plenachrome, Superpan Supreme, and Ultra Speed Panchromatic, manufactured by the Agfa Ansco Corporation; Micropan, Parpan, and

Superior Panchromatic, manufactured by the Du Pont Film Manufacturing Corporation; and Microfile, Panatomic X, Plus X, and Super XX Panchromatic, manufactured by the Eastman Kodak Company. Eastman D-76, Eastman DK-20, Champlin 16, and Harvey 777 Panthermic, widely used developers of different characteristics, were chosen as typical reducing solutions. All data listed were obtained from carefully prepared sensitometric strips developed to a gamma of 0.6 at the temperature recommended by the manufacturer of the developer and under uniform conditions of processing. The relative graininess of the films in the different developers was determined by a variation of the method described by Jones and Deisch and the relative speed by a gradient method of speed specification.

TABLE I. *Relative speed—graininess data for films developed in Eastman D-76 at 18°C.*

Film	Development Time	Gamma	Density	Fog	Speed	Graininess
Agfa Finopan	7.0 min.	0.60	0.37	0.00	0.29	0.84
Agfa Plenachrome	6.5 min.	0.58	0.42	0.01	0.21	0.87
Agfa Superpan Supreme	7.5 min.	0.59	0.30	0.03	0.84	0.94
Agfa Ultra Speed	14.0 min.	0.59	0.34	0.03	1.67	1.06
Dupont Micropan	5.0 min.	0.61	0.39	0.07	0.15	0.76
Dupont Parpan	9.0 min.	0.60	0.39	0.04	0.17	0.96
Dupont Superior	13.0 min.	0.60	0.39	0.10	0.84	1.14
Eastman Microfile	2.0 min.	0.60	0.47	0.01	0.01	0.58
Eastman Panatomic X	10.0 min.	0.60	0.43	0.02	0.35	0.87
Eastman Plus X	12.0 min.	0.60	0.46	0.05	0.78	0.88
Eastman Super XX	13.5 min.	0.60	0.31	0.05	1.00	1.00

B. Procedure

A particular film to be studied was placed in a specially designed "camera," given a graded series of exposures, and processed under constant conditions of temperature and agitation.

The "camera" was a light-tight metal box designed to expose four square centimeters of the film directly to the source of illumination at each exposure. The light source consisted of a 40-watt, 115-volt Mazda lamp enclosed in a compact housing with a four-centimeter square opening. The lamp was mounted in such a manner that only diffuse light reflected from the white inner walls of the housing could reach the "camera" from the lamp. In order to furnish a source of artificial daylight for the exposures, the voltage of the lamp was maintained at 110 volts by means of a variable resistance in series with a 120-volt storage battery, and a two-inch square number 78 (daylight) Wratten filter was placed over the aperture in the housing. In exposing the film the intensity of illumination was held constant and the time of exposure increased geometrically by a factor of two for each exposure. The exposure time was controlled by means of a rotating sector disk driven by a Telechron synchronous motor at the rate of one revolution per second. A 36° opening in the disk allowed light to pass through the aperture in the housing for one-tenth of each revolution, giving accurate exposures of one-tenth second each second. Because of the widely varying sensitivity of the films used, the intensity was increased or decreased for different films by changing the distance from the source to the camera, but for any given film the intensity was maintained constant.

The exposed film was then placed in a standard 35-millimeter Leitz Correx developing tank and developed in a typical solution for the time required to produce a gamma of 0.6 and at the temperature recommended by the manufacturer of the developer. During development the film was agitated continuously by means of an electrically driven agitator which caused the developing reel to make twelve oscillations per minute. After development the film was rinsed in water or in a chrome alum stop bath if recommended by the manufacturer, fixed in an acid hardening fixing bath (Eastman F-5), washed thoroughly in running water, and dried. Throughout development and the auxiliary processes the temperature of the solutions was held constant to within ±0.5°C by means of water baths. Especial care was taken to adhere strictly to the instructions of the manufacturer of film and developer during all the processes.

TABLE II. *Relative speed—graininess data for films developed in Eastman DK-20 at 18°C.*

Film	Development Time	Gamma	Density	Fog	Speed	Graininess
Agfa Finopan	7.0 min.	0.60	0.41	0.01	0.15	0.83
Agfa Plenachrome	7.5 min.	0.58	0.45	0.04	0.25	0.92
Agfa Superpan Supreme	11.0 min.	0.60	0.41	0.05	0.66	0.86
Agfa Ultra Speed	18.0 min.	0.60	0.35	0.12	1.18	1.01
Dupont Micropan	4.5 min.	0.61	0.46	0.14	0.05	0.78
Dupont Parpan	7.5 min.	0.61	0.41	0.09	0.10	0.93
Dupont Superior	17.5 min.	0.58	0.35	0.13	0.38	1.08
Eastman Microfile	2.3 min.	0.61	0.38	0.02	0.01	0.60
Eastman Panatomic X	11.0 min.	0.59	0.38	0.08	0.20	0.81
Eastman Plus X	11.5 min.	0.61	0.40	0.06	0.45	0.80
Eastman Super XX	17.0 min.	0.60	0.34	0.11	0.71	0.87

The opacity of each step on the sensitometric strip was then determined by means of a photronic cell densitometer. A specially prepared Weston Photronic cell, which permitted the film to be placed in contact with the ground glass surface of the cell, served as a current source for a low resistance, sensitive Leeds and Northrup galvanometer when the cell was illuminated. To assure direct contact between film and cell and to insure the use of the same part of the cell for all readings, a Bakelite plate with a five by ten millimeter rectangular aperture was pressed against the face of the cell by a set of springs. The source of illumination for the cell was a 6-volt Mazda bulb operated at 5.75 volts by means of a variable resistance in series with a 120-volt storage battery.

The optical density of each step on the sensitometric strip was obtained by observing the galvanometer deflections when light passed through the clear film and when light passed through the silver deposit and employing the definition for density,

$$\text{Density} = \log_{10} \frac{\text{incident light}}{\text{transmitted light}}.$$

Since the illumination falling on the film was constant, the characteristic curve was drawn by plotting density against the logarithm of exposure time. The contrast factor, or gamma, for the strip was then determined by measuring the slope of the linear portion of the curve.

Since the chemical fog varied considerably for the different films, the density of the fog deposited on each strip was computed by taking the common logarithm of the ratio of the light transmitted through an undeveloped, fixed, and washed strip, to the light transmitted through an unexposed portion of the given strip.

TABLE III. *Relative speed—graininess data for films developed in Champlin 16 at 22.8°C.*

Film	Development Time	Gamma	Density	Fog	Speed	Graininess
Agfa Finopan	7.5 min.	0.60	0.31	0.02	0.11	0.80
Agfa Plenachrome	8.0 min.	0.61	0.32	0.02	0.21	0.89
Agfa Superpan Supreme	11.5 min.	0.61	0.40	0.04	0.60	0.87
Agfa Ultra Speed	15.5 min.	0.61	0.31	0.11	1.92	1.11
Dupont Micropan	7.2 min.	0.61	0.48	0.15	0.12	0.86
Dupont Parpan	9.0 min.	0.58	0.32	0.08	0.11	0.89
Dupont Superior	15.5 min.	0.59	0.36	0.21	0.66	1.13
Eastman Microfile	2.5 min.	0.59	0.47	0.02	0.01	0.56
Eastman Panatomic X	9.5 min.	0.61	0.42	0.04	0.30	0.94
Eastman Plus X	12.0 min.	0.60	0.48	0.07	1.00	0.93
Eastman Super XX	15.5 min.	0.60	0.31	0.12	1.19	1.04

TABLE IV. *Relative speed—graininess data for films developed in Harvey 777 Panthermic at 23°C.*

Film	Development Time	Gamma	Density	Fog	Speed	Graininess
Agfa Finopan	5.8 min.	0.60	0.48	0.01	0.10	0.83
Agfa Plenachrome	8.2 min.	0.61	0.38	0.03	0.29	0.84
Agfa Superpan Supreme	9.5 min.	0.60	0.30	0.05	0.40	0.89
Agfa Ultra Speed	12.5 min.	0.60	0.37	0.08	1.08	1.04
Dupont Micropan	3.8 min.	0.60	0.36	0.15	0.09	0.78
Dupont Parpan	5.8 min.	0.60	0.40	0.12	0.07	0.87
Dupont Superior	12.5 min.	0.58	0.47	0.23	0.55	1.13
Eastman Microfile	2.0 min.	0.60	0.40	0.02	0.01	0.57
Eastman Panatomic X	12.0 min.	0.61	0.38	0.08	0.30	0.87
Eastman Plus X	9.2 min.	0.59	0.38	0.06	0.40	0.80
Eastman Super XX	10.0 min.	0.60	0.31	0.07	0.51	0.95

In the determination of the relative emulsion speeds of the different films in different developers, the exposure at which the gradient of the characteristic curve was 0.3 was taken as an index of measurement and the speed of Eastman Super XX developed in Eastman D-76 was arbitrarily chosen as unity. All other emulsion speeds were compared with this value as a standard by dividing the exposure corresponding to a gradient of 0.3 on the curve of the standard by the exposure corresponding to the same gradient on the curve of the film under consideration.

The graininess of the films was determined by a variation of the method described by Jones and Deisch. A set of photomicrographs, with a magnification of 300 diameters, was prepared from a representative portion of the deposit on each sensitometric strip with a density of approximately 0.4 and printed on Azo number 4 glossy paper. The prints were exposed so that all appeared to have the same density when viewed from beyond their merging distances and were developed to the same contrast under uniform conditions of processing. The matched, $2\frac{1}{4}$-inch square prints were mounted upon a white board and uniformly illuminated for viewing. The distance at which each photomicrograph blended into a homogeneous area was determined by twenty randomly selected observers, and, to eliminate differences in the visual acuity of the observers, the graininess of Eastman Super XX developed in Eastman D-76 was arbitrarily chosen as unity. The graininess of each deposit was compared with this value as a standard by dividing the blending distance of the photo-

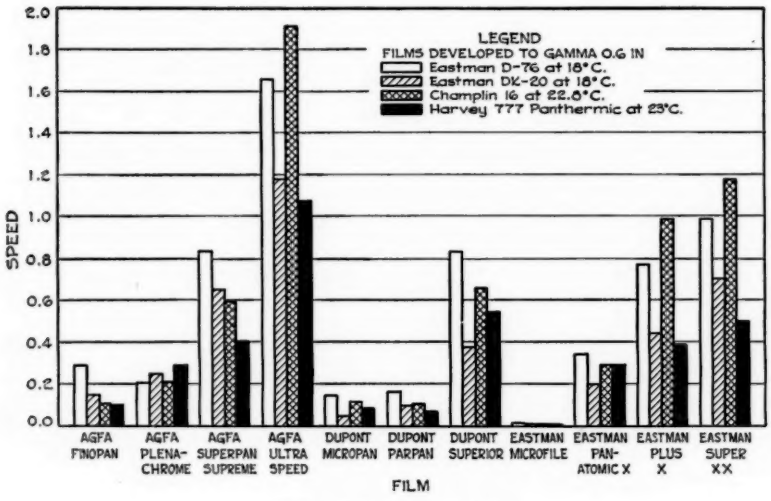

FIG. 1. Relative speed data.

micrograph of that deposit by the blending distance of the standard.

C. Results

The results of the study of the fogging effect of the developers and the relative emulsion speeds and graininess of the various films developed in D-76, DK-20, Champlin 16, and Harvey 777 are listed in Tables I, II, III, and IV, respectively. The relative speeds were obtained directly from the characteristic curves, while the values for relative graininess are the average of the results of the twenty observers. For convenience of study, the same data on relative speed and relative graininess are represented graphically in Figs. 1 and 2. A statistical study of the accumulated data shows a probable error of 0.05 in the graininess results.

IV. Discussion

For convenience in the discussion, the films tested may be divided into three general groups, namely, (1) fast films with relative speeds greater than 0.4, (2) moderately fast films with speeds between 0.2 and 0.4, and (3) slow films with speeds less than 0.2. A study of Fig. 1 indicates that Superpan Supreme, Ultra Speed, Superior, Plus X, and Super XX fall into group 1; Finopan, Plenachrome, and Panatomic X into group 2; and Micropan, Parpan, and Microfile into group 3. A similar study of Fig. 2 shows that, in general, the emulsions included in group 1 have the coarsest grain structure, those in group 2 slightly less graininess, and slow emulsions of group 3 decidedly finer grain structure. Of course, the divisions between the groups are not sharp, and there are exceptions to this generality. For instance, Plus X has a graininess comparable to the films of group 2 and Parpan, an exceedingly slow emulsion, has a coarse grain structure.

The differences in graininess produced by the four developers in a given film are only slight in comparison with the inherent differences among the various films. The relative graininess obtained with DK-20 and Harvey 777 is definitely less than that produced by D-76 for all the films of group 1, but these developers are decidedly less effective for the films of groups 2 and 3. For these emulsions slight differences in density and contrast may completely obscure the effects of the developers. In all cases, decreased graininess is obtained only at the sacrifice of effective emulsion speed. These results are in agreement with the work of van Kreveld and Scheffer[16] and Higgins,[8] who definitely concluded that fine-grain developers were more effective in reducing the graininess in fast, coarse-grain emulsions than in slow, fine-grain emulsions.

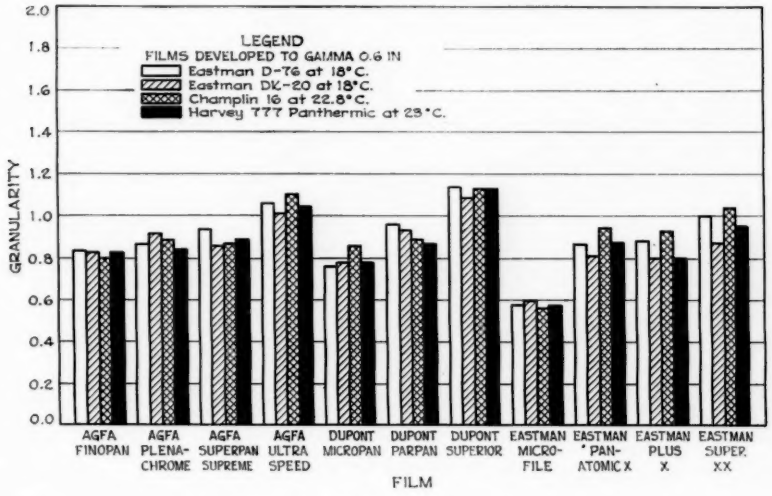

FIG. 2. Relative graininess data.

When the films are developed to a gamma of 0.6, Champlin 16 is ineffective in reducing graininess. In several cases the graininess is actually greater than that produced by D-76, particularly with the fast, coarse-grain emulsions; in these cases, however, there is a corresponding increase in effective emulsion speed. The development times recommended by Champlin[1] are insufficient to produce a practical contrast at the temperatures suggested, and under these conditions a fine-grain structure is obtained at the expense of contrast and tonal quality.

The fogging effect of the different developers varies considerably, the fog produced by DK-20, Champlin 16, and Harvey 777 being consistently denser than that produced by D-76.

V. Conclusions

The results of this investigation on the graininess and speed of various types of photographic films indicate that for the films and developers considered:

(1) The differences in graininess produced by fine-grain developers are only slight in comparison with the inherent differences among the various films. (2) Fine-grain developers are effective in reducing the graininess of fast, coarse-grain emulsions. (3) Fine-grain developers are only slightly effective in reducing the graininess of slow, fine-grain emulsions, and slight differences in density or contrast may completely obscure the effects of the developers. (4) Reduced graininess can be obtained only at the sacrifice of effective emulsion speed. (5) Reduced graininess may be obtained at the expense of contrast and tonal quality. (6) The fogging effect of fine-grain developers is greater than the fogging effect of a typical elon-hydroquinone developer.

Acknowledgments

The writer wishes to express his gratitude and indebtedness to Dr. P. H. Carr for the many valuable suggestions and helpful criticisms which he made while directing this investigation, and to Dr. J. W. Woodrow for providing the photographic materials and apparatus used in this investigation. He also wishes to thank the members of the physics staff who served as observers for the measurements on graininess.

Selected References

1. Harry Champlin, *Champlin on Fine Grain* (Camera Craft Publishing Company, 1938), pp. 91–102.
2. O. E. Conklin, "Some applications of the comparison microscope in the film industry," J. Soc. Mot. Pict. Eng. **16**, 159–167 (1931).
3. J. I. Crabtree, "The maintenance of negative quality," Am. Phot. **13**, 800–804, 874–880 (1937).

4. A. Dember, A. Goetz and W. O. Gould, "The objective quantitative definition of the graininess of photographic emulsions," Phys. Rev. **54**, 240 (1938).
5. F. L. English, "Some factors affecting grain size," Am. Phot. **31**, 305–315 (1937).
6. A. Goetz and W. O. Gould, "The objective quantitative determination of the graininess of photographic emulsions," J. Soc. Mot. Pict. Eng. **29**, 510–538 (1937).
7. A. C. Hardy and L. A. Jones, "Graininess in motion picture negatives and positives," Trans. Soc. Mot. Pict. Eng. **14**, 107–119 (1922).
8. George Higgins, "Fine grain photographic development," J. App. Phys. **10**, 18–26 (1939).
9. M. B. Hodgson, "The physical characteristics of the elemental grains of a photographic plate," J. Frank. Inst. **184**, 705–715 (1917).
10. L. A. Jones, "The evaluation of negative film speeds in terms of print quality," J. Frank. Inst. **227**, 297–354, 497–544 (1939).
11. L. A. Jones, "*Photographic Sensitometry*," (Eastman Kodak Company, Rochester, New York).
12. L. A. Jones and N. Deisch, "The measurement of graininess in photographic deposits," J. Frank. Inst. **190**, 657–683 (1920).
13. L. A. Jones and C. N. Nelson, "A study of various sensitometric criteria for negative film speeds," J. Opt. Soc. Am. **30**, 93–109 (1940).
14. L. A. Jones and M. E. Russell, "Minimum useful gradient as a criterion of photographic speed," J. Opt. Soc. Am. **25**, 396–411 (1935).
15. A. van Kreveld, "Objective measurements of graininess of photographic materials," J. Opt. Soc. Am. **26**, 170–176 (1936).
16. A. van Kreveld and J. C. Scheffer, "Graininess of photographic materials in objective absolute measure," J. Opt. Soc. Am. **27**, 100–109 (1937).
17. E. M. Lowry, "An instrument for the measurement of the graininess of photographic materials," J. Opt. Soc. Am. **26**, 65–72 (1936).
18. A. and L. Lumière, and W. Seyewetz, "The influence of the character of developers on the size of grain of reduced silver," Brit. J. Phot. **51**, 630–631 (1904).
19. J. E. Mack and M. J. Martin, *The Photographic Process* (McGraw-Hill, New York, 1939), pp. 156–197; 199–219.
20. A. Marriage, "A note on the effect of processing conditions on graininess," Phot. J. **77**, 379–380 (1937).
21. C. B. Neblette, *Photography, Its Principles and Practice* (D. Van Nostrand Company, New York, 1935), pp. 149–167; 209–239.
22. V. Ronchi, "Measurement and specification of 'grain' of photographic emulsions," Ricerca Scient. **2**, 588–596 (1938). Original not seen. Abstract in Sci. Abst. **A42**, 276 (1939).
23. G. Schwarz, "Fine-grain emulsions, fine-grain developers, and sensitivity," Kinotech. **19**, 51–53 (1937). Original not seen. Abstract in Chem. Abst. **32**, 64 (1938).
24. E. W. H. Selwyn, "A theory of graininess," Phot. J. **75**, 571–580 (1935).
25. S. E. Sheppard, and C. E. K. Mees, *Investigations on the Theory of the Photographic Process* (Longmans, New York, 1909).
26. S. D. Threadgold, "Measurement of graininess," Phot. J. **72**, 348–351 (1932).
27. C. Tuttle, "Methods and instruments for the determination of photographic speeds by measurement of relative characteristic gradients," J. Opt. Soc. Am. **29**, 267–277 (1939).
28. R. J. Wallace, "The silver grain in photography," Astrophys. J. **20**, 113–122 (1904).

Scattering of Light by Pigment Particles

DAYTON H. CLEWELL*
Magnolia Petroleum Company, Dallas, Texas
(Received May 5, 1941)

INTRODUCTION

THE ability of turbid media to diffuse light has interested the physicist ever since the advent of the Maxwell electromagnetic theory. The late Lord Rayleigh formulated a successful mathematical theory of scattering wherein he arrived at the familiar inverse fourth power of wave-length law. His law has been proven correct in numerous places and its only restriction is that the particles be small compared to the wave-length of the incident light. Partially to overcome this restriction Lord Rayleigh extended his first formulation to include particles whose diameter was of the same order as the wave-length of the light, but in so doing he had to assume that the relative index of refraction between particle and medium was very close to unity. This assumption allows the incident wave front to flow through the particulate medium as a smooth and unbroken surface since the retardation of the light passing through any individual particle will not be sufficiently retarded to render it appreciably out of phase with the light which passes by in the immediate neighborhood of the particle.

In many instances of great practical importance the particles of the diffusion media are neither small in diameter nor approach unity in relative index of refraction. The paint and pigment manufacturers are very well acquainted with the fact that maximum optical effects are to be obtained when the relative index of refraction is as large as possible and the pigment particle diameter is in the neighborhood of one-half the wave-length of visible light. Since the ordinary optical properties of pigments, opacity, brightness and color, are determined by the absorption coefficient and the scattering coefficient of the material, and since it is difficult to reason that particle size will influence the absorption coefficient μ, it is generally assumed the wide variations in optical properties of a particulate medium caused by variations in the size of particles result from a dependence of the scattering coefficient S on the particle size.

In attempts to evolve a working rule that would enable the writer to predict this dependence of scattering on particle size of commercial pigments an empirical equation was formulated which in a qualitative way has been quite useful. The equation was constructed by simply selecting an algebraic expression which would fit the experimental data as closely as possible. No rigorous theoretical justification of the equation was attempted. No effort was made to extend the already complex Rayleigh equations into regions of even greater mathematical complexity, but it was required that the empirical formula reduce to the correct Rayleigh scattering in the proper regions. The remainder of this discussion is concerned with the steps by which the empirical formulation was made.

For reasons of consistency and utility it will always be assumed that the mass concentration of pigment per unit volume of vehicle will be held constant; that is, if the particle diameter is increased, the number of particles will decrease by the necessary amount to keep the concentration constant and vice versa.

In any consideration of the scattering of light by particles whose diameters may range from 0.1λ to 20λ (λ = wave-length of light) perhaps the most obvious fact to be noted is that there must be a maximum of scattering for a range of diameters lying between the extreme sizes. In the region of very large particles scattering is caused by the regular reflection of the light at the surface of the particle. In such cases the surface area is proportional to $1/d$ and likewise S is proportional to $1/d$ (d = particle diameter) and the scattering *increases* as the pigment is made *finer*. On the other hand, in the region of very small particles the Rayleigh law[1] states that the scattering S is proportional to d^3/λ^4 from which it is obvious that the scattering increases as the

*Formerly with C. K. Williams Company, Easton, Pennsylvania, where this work originated.

[1] Lord Rayleigh, Proc. Roy. Soc. **A90**, 219 (1914).

pigment is made *coarser*. In the transition range there must, therefore, be a maximum, whose position will be a function of λ as well as of d.

The maximum is shown experimentally in Fig. 1 which is the measured green transmission of a number of water suspensions of ZnO of varying particle size, but always of equal concentration by weight of ZnO. This curve was obtained by Stutz and Pfund[2] using a turbidimetric method of measurement. Their experiment consisted of measuring the specular transmission of parallel light incident upon the ZnO suspension. The intensity measurements were made with the use of an optical pyrometer in conjunction with a green filter whose dominant wave-length was around 0.54μ. Since the ZnO particles are transparent the effect of absorption on measured transmission is very small and the minimum transmission is a result of a maximum of scattering.

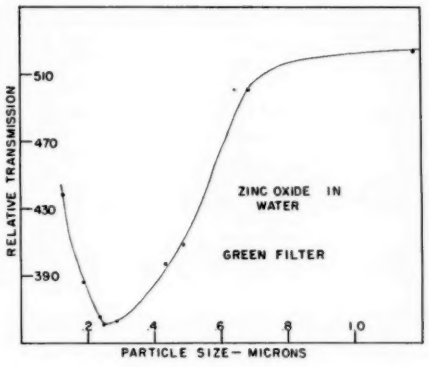

FIG. 1.

RAYLEIGH SCATTERING

The complete Rayleigh formula for the intensity of light scattered by a single spherical particle illuminated by radiation of unit intensity is

$$S'_{(\varphi,\chi)}=\frac{\pi\alpha^4 d^2\eta}{8r^2m^3}[1-\sin^2\chi\cos^2\varphi]J_{3/2}{}^2(m), \quad (1)$$

where χ is the angle between scattered and incident radiation; φ, the angle between scattered radiation and plane of polarization; r, the distance from particle; d, the particle diameter; n_0, index of refraction of vehicle; n, index of refraction of particle relative to vehicle; λ, wave-length of radiation; $\alpha=\pi dn_0/\lambda$; $m=2\alpha\cos\frac{1}{2}\chi$; and $\eta=9[(n^2-1)/(n^2+2)]^2$.

This formula is applicable only for cases where $(n^2-1)d/2\lambda$ is small; that is, it is applicable for any value of n if d is small compared to λ, but good only for values of n close to unity if d and λ are of the same order of magnitude.

Integration of Eq. (1) over all values of χ and φ to obtain the total amount of scattering by a particle illuminated with an unpolarized beam of unit intensity has been shown by Rayleigh to yield

$$S'\sim\eta d^6/(\lambda/n_0)^4,$$

when d/λ is small, and to yield

$$S'\sim\eta d^4/(\lambda/n_0)^2,$$

when n is nearly equal to unity and d is of the same order of magnitude as λ.

If it is assumed that the scattering for N particles is N times the scattering for one particle and if it is also required that the mass concentration of scattering material be independent of d the above two expressions become

$$S=NS'\sim\eta d^3/(\lambda/n_0)^4; \quad d/\lambda\ll 1 \quad (2)$$

$$S=NS'\sim\eta d/(\lambda/n_0)^2; \quad n\leqq 1. \quad (3)$$

In the development of the Rayleigh relations it is always assumed that the primary beam, which is not scattered, is not sufficiently retarded during its passage through the particle to interfere destructively with the light passing by in the immediate neighborhood of the particle. In other words, the particle does not appreciably interfere with the wave front since it is either assumed small or it is assumed to have a relative index of nearly unity if it is large.

The problem now resolves itself into the determination of a formula which will correctly predict the location of the experimental maximum of scattering in Fig. 1 and at the same time harmonize with the two forms of the simple Rayleigh law expressed by Eqs. (2) and (3). This formula should also indicate that regular reflection proportional to surface area accounts for scattering by very large particles.

[2] G. F. A. Stutz and A. H. Pfund, Ind. Eng. Chem. **19**, 51 (1927).

Diffraction Scattering

In the situation intermediate scattering by regular reflection and Rayleigh scattering the particles *are not* large enough to reflect incident light regularly but *are* of sufficient size to break up the wave front of incident radiation when their relative index of refraction is large.

The particle becomes a new source for the incident radiation passing through and this radiation will now spread by diffraction. The scattering by diffraction will be very intense since it involves all the light which strikes the particle.

The interesting point about most pigment particles is that they show a maximum of scattering (Fig. 1) when the particle diameter is approximately $\lambda/2$, a size that coincides with the ultimate resolving power of a microscope. The agreement is not an accident since it is also diffraction which determines resolving power.

Abbe, in discussing the resolving power of microscopes, has shown that a particle becomes unresolvable when its diffraction pattern has been spread out into a cone whose apex angle is 180° and can no longer be entirely collected by the objective of the microscope. This is obviously the same size particle that is capable of scattering the maximum amount of light. If the particle becomes still smaller, less radiation is incident upon it to become available for scattering and if it is larger it diffracts the radiation into a smaller cone.

It was, therefore, thought that diffraction scattering should be considered the predominating phenomenon in the transition range between Rayleigh scattering and scattering by regular reflection. Attempts were made to develop an empirical equation embodying the idea as follows:

Diffraction theory shows that a particle of diameter d immersed in a medium of index n_0 will diffract a ray of light into a cone whose half-apex angle θ is given by the relation

$$\sin\theta = 0.61\lambda/n_0 d$$

and maximum scattering will occur when $\theta = \pi/2$, or

$$0.61\lambda/n_0 d = 1.$$

From the curve of Fig. 1 it is noticed that the observed scattering is a function which somewhat resembles the response of a natural oscillator under the influence of an impressed sinusoidal force. Using the equation of a natural oscillator as a model, the function S was represented as

$$S \sim \frac{1/d}{[(0.61\lambda/n_0 d)^2 - 1]^2}, \tag{4}$$

where $(0.61\lambda/n_0)$ and d are analogous, respectively, to the impressed and natural frequencies of an oscillator.

The factor $1/d$ was introduced since for a constant weight of material the surface area of the pigment determines how much radiation will strike a particle and be made available for scattering.

Equation (4) already reduces to the correct values for very large or very small particles since when d is large the denominator becomes unity and when d is small unity can be neglected and the scattering is proportional to d^3/λ^4. The equation also gives the required maximum of scattering when the particle is diffracting most efficiently. It is immediately evident, however, that the scattering cannot be infinite at the maximum. Infinite scattering is impossible since the undeviated radiation transmitted by the particle will never be completely independent of the unobstructed radiation passing by in the region immediately adjacent to the particle. Equation (4) was modified to take care of this condition by the introduction of what may be termed a "damping" constant α

$$S \sim \frac{1/d}{[(0.61\lambda/n_0 d)^2 - 1]^2 + \alpha}. \tag{5}$$

A consideration of α shows that it should measure the degree to which the transmitted light is out of phase with the original incident light and can, therefore, be a complicated function itself. However, it plays an important role only in the immediate neighborhood of the maximum.

If the transmitted light has been retarded a half-wave, α should be small, while if the retardation has been zero, α should be large. Let n equal the relative index of refraction and ρ equal the number of wave-lengths the transmitted ray

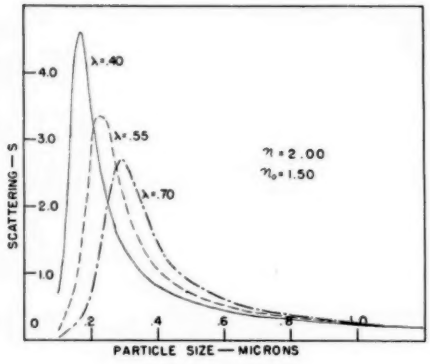

FIG. 2.

is retarded. Then,

$$\rho = n_0 d(n-1)/\lambda$$

and it seems reasonable that α should be some inverse function of ρ since when ρ is large the probability of the particle breaking up the wave front is high. One might reason that a retardation of a full wave-length should be equivalent to zero retardation but this is very unlikely in any real particle because any particle capable of retarding the transmitted radiation a full wave-length will very likely have a plurality of transmission paths whose retardations vary all the way from zero retardation for a short path to a maximum retardation at the thickest section.

One of the requirements of Eq. (5) is that it reduce to the Rayleigh formula (3) when $n \leqq 1$, a requirement that is nearly fulfilled if

$$\alpha = \frac{1}{\rho^2} = \frac{\lambda^2}{n_0^2 d^2 (n-1)^2}.$$

This expression for α is not wholly correct as it stands since α will approach infinity as n approaches unity. This singularity can be prevented by the introduction of a constant a such that

$$\alpha = \frac{\lambda^2}{n_0^2 d^2 a[(n-1)^2 + 1/a]},$$

where now α is $\lambda^2/n_0^2 d^2$ when the relative index is unity.

Equation (5) was accordingly transformed to

$$S \sim \frac{[(n^2-1)/(n^2+2)]^2}{d[(0.61\lambda/n_0 d)^2 - 1]^2 + \lambda^2/\{n_0^2 da[(n-1)^2 + 1/a]\}}, \quad (6)$$

where the factor $[(n^2-1)/(n^2+2)]$ was introduced to maintain agreement with the Rayleigh formula. Equation (6) is thus offered as a semi-empirical solution to the problem of scattering of light by pigments because it predicts the experimentally observed scattering maximum, reduces to something proportional to surface area for large values of d, reduces to Eq. (2) for small values of d, and finally it also reduces to Eq. (3) for values of d comparable to λ (i.e., $0.61\lambda/n_0 d \leqq 1$) when the relative index approaches unity.

In passing it should be noted that diffraction can occur in two ways since the particle serves both as an "aperture" and a "stop" for either of which the diffraction is equivalent. Even if the particle is completely opaque it can diffract because it serves as a "stop." The function of the particle as a "stop" indicates that at the scattering maximum the sphere of influence of the particle is greater than the actual physical size of the particle.

CHARACTERISTICS OF DIFFRACTION SCATTERING

Equation (6) has been plotted as a function of d for various values of n and λ in Figs. 2, 3 and 4. The first characteristic to be noted is that the experimentally observed maximum of scattering in the particle size range around 0.25 micron is predicted. If the particle size is below 0.6 micron, it is observed that the scattering is selective with wave-length, the selectivity decreasing as n decreases. Between 0.6 micron and 0.25 micron the longer wave-lengths of the visible spectrum are scattered *more* than the shorter ones (see Figs. 2 and 3).

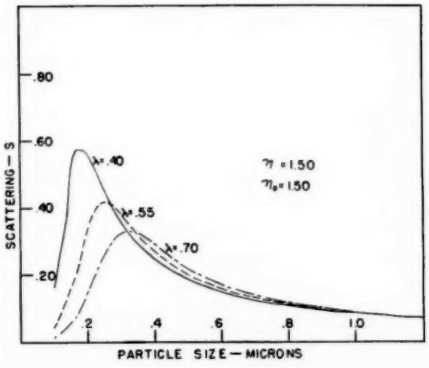

FIG. 3.

If n is sufficiently large, it is possible for green scattering to be greater than either blue or red scattering for particle sizes in a narrow range around 0.25 micron (Fig. 2). Below about 0.22 micron the blue scattering predominates and continues to do so all the way down to infinitely small particles. For values of n approaching unity the second term in the denominator of Eq. (6) controls the scattering in the potential diffraction range to such an extent that short wave-length scattering will predominate for all particle sizes. This characteristic is illustrated in Fig. 4 where it will be noted that red and green scattering is everywhere less than the blue scattering.

In any suspension of pigment particles it will be a very rare occasion when all the particles are of the same size. If they should all be of the same size, the observed scattering will be very selective with wave-length; and if the relative index is high, green scattering can greatly predominate over the red and blue scattering. If the pigment is not uniform in size the total scattering must be found by an integration of the product of the scattering function with the size distribution function. It is immediately evident that the particles in the diffraction range will exercise the main control of the optical properties of the pigment. In general a lack of uniformity will decrease the wave-length selectivity of the scattering.

The question arises as to which of the many particle diameters that can be assigned to a pigment should be used in Eq. (6). Rayleigh scattering is a volume effect and in this range the D diameter should be used since from it the total volume or weight of the pigment is calculated. In the diffraction range the arithmetical mean diameter d_1 should be used since diffraction depends on the linear dimensions of the particle. In the regular reflection range d_3 should be used since it is a measure of surface area. As the pigment becomes more and more uniform in particle size the various diameters become equal.

The point of maximum scattering is nearly independent of the relative index of the particles but shifts with the index of the suspending medium.

Experimental Evidence

The experimental verification of Eq. (6) on an accurate quantitative basis becomes difficult since it requires a precise and absolute measurement of particle size. Direct measurements of particle sizes in the region where they are just resolvable by a microscope are at present unreliable in absolute value.

The scattering function described by Eq. (6) differs from other scattering functions in that it

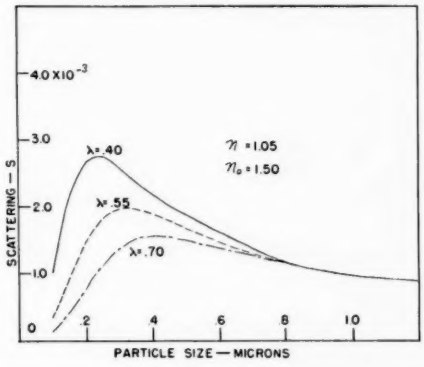

FIG. 4.

predicts the possibility of scattering the red end of the spectrum with greater efficiency than the blue end, provided the relative index of the particles is sufficiently high to make diffraction scattering predominate over d/λ^2 type of Rayleigh scattering. Experimental evidence of red scattering would thus qualitatively verify this proposed function.

Red scattering has been observed in a number of cases; Stutz and Pfund in the experiments they carried out to determine the curve of Fig. 1 observed that the opacity of their zinc oxide suspension was greater for red than for blue light when their particles were larger than those which gave the maximum opacity. If the particles were finer than the optimum size blue light was scattered more than red. Thus, by using blue and red filters, it was possible for them to determine quickly on which side of the point of minimum transmission a particular pigment was located.

A still better confirmation of the Eq. (6) is provided by the data[3] of Fig. 5 which is a more

[3] Data obtained through courtesy of New Jersey Zinc Company, Palmerton, Pennsylvania.

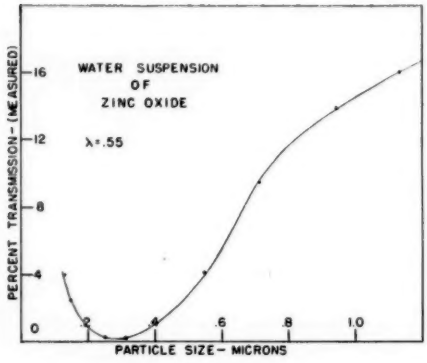

FIG. 5.

precise presentation of the phenomenon represented by Fig. 1. In Fig. 5 the measured specular transmissions of a series of zinc oxide suspensions are plotted as a function of the particle size of each suspension. It should, of course, be pointed out that all the particles of each suspension were not necessarily of the same size, although zinc oxide suspensions are much more uniform in particle size than most pigment suspensions. Assuming that the transmission in the absence of absorption is related to the scattering coefficient S by the relation

$$T=e^{-Sx},$$

where x is the thickness of the suspension and T is the percentage transmission, the curve of Fig. 5 can be translated to curve C of Fig. 6 in which S is plotted as a function of d.

In the water suspensions of zinc oxide $n_0=1.33$, $n=1.50$ and $\lambda=0.55\mu$ and by substituting these values into Eq. (6) and selecting a value of $a=7$, the curve A of Fig. 6 is obtained. By choosing $a=6$, the curve B is determined. All the curves have been adjusted to coincide at $d=0.75$ micron. It is significant that both curves A and B agree with the experimental curve in regard to the position of the scattering maximum. It is possible that curve A with $a=7$ is to be preferred over curve B since the non-uniformity of particle size in the experimental suspensions can explain the difference between curve C and A. Non-uniformity can be taken into account by multiplying Eq. (6) by the size distribution function of the suspended particles and integrating the product between the particle size limits existing in each suspension. Non-uniformity will attenuate the maximum of scattering and the presence of fines in the coarse suspensions will increase the scattering of these suspensions above the theoretical value for uniform particles. It is likely that curve A would agree even more closely with curve C if the size distribution were considered.

Keen and Porter[4] performed the well-known experiment of precipitating sulphur out of an acidified sodium thiosulphate solution.[5] As the sulphur particles grew in size, the usual Rayleigh blue scattering was observed. However, as the particles came into the diffraction range, where their diameter was approximately $\lambda/2$, it was observed that the blue scattering gave way to green scattering which in turn quickly changed to red scattering, rapidly followed by non-selective or white scattering. The relative index of sulphur in water is high enough to take the suspension out of the d/λ^2 Rayleigh range. The observable green scattering was probably due to a high degree of uniformity.

R. W. Wood reports, in his book on physical optics,[6] observing what is termed a resonant scattering effect. His experiment consisted of condensing sodium vapor on to a glass surface in vacuum. The condensed sodium was made up of fine particles widely separated from one another on the glass surface. It was observed that certain regions of the deposit were either blue, green or red when observed by light which was scattered. It is believed that the high uniformity which very probably prevailed within certain regions made it possible for these particles to very efficiently scatter the radiation for which $0.61\lambda/n_0d$ was equal to unity.

Further qualitative verification of Eq. (6) has been observed in connection with the color of opaque pigments. If an opaque pigment suspension is illuminated with diffuse light, Ryde[7] calculates its reflection factor to be

$$R=NB/(\mu+NB)+[\mu(\mu+2NB)]^{\frac{1}{2}}.$$

The term NB may be considered the scattering coefficient S_0 of the pigment suspension though it

[4] B. A. Keen and A. W. Porter, Proc. Roy. Soc. **A89**, 370 (1913).

[5] Jerome Alexander, *Colloid Chemistry* (Chemical Catalog Company, New York, 1926), Vol. I, p. 356.

[6] R. W. Wood, *Physical Optics* (Macmillan Company, New York, 1934), third edition, p. 436.

[7] J. W. Ryde, Proc. Roy. Soc. **A131**, 451 (1931).

is not the same as S since S_0 describes only the ability of the particles to scatter light backwards, whereas S describes the total scattering ability of the particles. If μ is very large, R approaches a condition of being linearly proportional to S_0 and the color of the pigment is largely determined by the scattering. As an example of the influence of scattering on color, the writer has had occasion to observe the color changes that accompany an alteration of the fineness of a dark colored pigment. This particular pigment, when it is very coarse, exhibits a reddish purple color; i.e., its green reflectance is slightly lower than the blue reflectance, while both are lower than the red reflectance. As this pigment is increased in fineness to a point where a large number of the particles are in the neighborhood of 0.3 micron, it is found that the green brightness rises considerably faster than the blue and eventually exceeds it. The purple color disappears and an orange-red results. The color of the coarse pigment is undoubtedly determined almost entirely by μ since its scattering is nonselective. The color change which accompanies the increase in fineness must certainly require, therefore, a selective scattering phenomenon which allows the longer wave-lengths to be scattered more than the shorter.

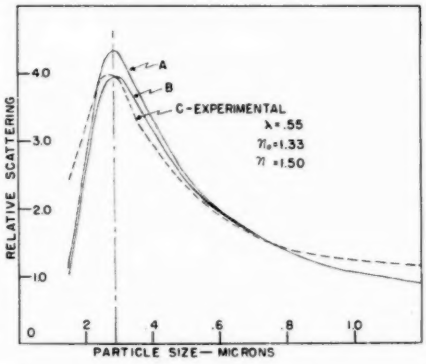

FIG. 6.

CONCLUSIONS

With very little theoretical justification, a scattering function has been empirically derived which attempts qualitatively to describe scattering as a function of particle size over a wide range of sizes and of indices of refraction. Diffraction scattering, if considered the basic phenomenon in the regions of extreme scattering such as exhibited by fine high index pigments, immediately accounts for the fact that all pigments whose size range is in the neighborhood of $\lambda/2$ for visible light possess a maximum of scattering.

This scattering function was found to reduce to the two types of Rayleigh scattering; namely, to d^3/λ^4 for small particles and to d/λ^2 for large particles of very low index, and to reflection scattering, $1/d$, for very large particles. The function predicts the possibility of long wave-lengths being scattered with greater efficiency than short ones, by particles ranging in size from 0.3 to 0.5 micron.

Considerable experimental evidence justifies the proposed scattering function in a qualitative manner, particularly in support of the red scattering.

Before Eq. (6) can be accepted with any assurance of its quantitative value, considerable experimentation remains to be done. It is, therefore, now offered simply as a useful guide in predicting the dependence of scattering on particle size.

Penetration of Fog by Light from Sodium and Tungsten Lamps

MATTHEW LUCKIESH AND L. L. HOLLADAY
Lighting Research Laboratory, General Electric Company, Nela Park, Cleveland, Ohio
(Received May 3, 1941)

A NUMBER of investigations have dealt with the influence of wave-length of light upon its ability to traverse atmospheres laden with fog and moisture. Some of these investigations have been made on natural fogs and the others on artificial ones. Among the chief investigations of the spectral transmissions of artificial fogs are those of Utterback,[1] Anderson,[2] and Houghton.[3] From analyses of these results by Stratton and Houghton,[4] Breckenridge[5] and others it has been found that the particle size of the fog is a controlling factor in the transmission characteristics of the fog and that the manner of its production may influence the particle size.

Among the chief investigations of the spectral transmission of natural fogs are those of Karrer and Tyndall,[6] Benford,[7] and Granath and Hulburt.[8] Karrer and Tyndall made transmission measurements of natural fog for light traversing a wooded terrain, about 2000 feet wide, and reflected back to a spectrophotometer. Measurements were made in various kinds of weather during April and May. A somewhat similar investigation of natural fog over a distance of 2300 feet was made by Benford. Granath and Hulburt reported transmission measurements of a 1300-foot stretch of fog along the bank of a large river. Their determinations were made by the use of a spectrograph and thermopile. These investigations show an increase in the transmission of natural fog with increase of wave-length from the blue to the red end of the visible spectrum. General averages of these relative transmissions for similar weather conditions are presented in Table I. Each transmission value of each of these three investigations has been expressed as a percent of the transmission of the sodium D_2 line at λ5890.

These data show progressive trends and a reasonable consistency. However, the magnitude of the selectivity is scarcely great enough to warrant some of the claims made for yellow light at least without the support of actual comparative measurements of visibility. For example, so-called fog-lamps, consisting of yellow lenses which absorb from 20 to 35 percent of the tungsten-filament light, have been commercialized for years. Obviously to be worth while they must contribute something toward seeing to offset the loss due to less light. In other words, the visibility of an object or of the lamp must, at least, be as great with the yellow light of lesser intensity as with the original tungsten-filament light of greater intensity. Only accurate measurements of visibility can determine this and no entirely satisfactory ones have been published.

Similar claims have been made for light from present-day sodium lamps. In this case there is

TABLE I. *Relative spectral transmissions of the earth's atmosphere during various kinds of weather, based on averages of measurements by Karrer and Tyndall, Benford, Granath and Hulburt, and Fowle.**

Wave-Length (Angstroms)	Average Relative Transmission				
	Clear	Hazy	Very Foggy	High Humidity	Snowing
4000	89	76	57	—	—
4300	93	85	68	65	—
4600	96	91	77	75	71
5000	98	94	86	85	78
5890	100	100	100	100	100
6300	101	103	103	105	109
6600	103	105	105	110	—
7000	104	115	107	—	—
8000	106	—	110	—	—

* F. E. Fowle, *Smithsonian Physical Tables* (The Smithsonian Institution, 1934).

[1] C. L. Utterback, "Transmission of Colored Light through Fog," Trans. I. E. S. **14**, 133 (1919).
[2] S. H. Anderson, "Transmission of Light through Fog," Aviation **28**, May 10, 1930.
[3] H. G. Houghton, "Transmission of Visible Light through Fog," Phys. Rev. **38**, 152 (1931).
[4] J. A. Stratton and H. G. Houghton, "A Theoretical Investigation of the Transmission of Light through Fog," Phys. Rev. **38**, 159 (1931).
[5] F. C. Breckenridge, "Transmission of Light through Fog," Proc. I. I. C. **1**, 463 (1931).
[6] E. Karrer and E. P. T. Tyndall, "Relative Spectral Transmission of the Atmosphere," Scientific Paper, Bureau of Standards No. 389 (1920), p. 377 and 396.
[7] F. Benford, "Projection of Light," Gen. Elec. Rev. **29**, 873, December 1926.
[8] L. P. Granath and E. O. Hulburt, "Absorption of Light by Fog," Phys. Rev. **34**, 140 (1939).

no loss of light by colored filters for the light is inherently yellow and practically monochromatic. In considering the greater scattering or absorption of light of wave-lengths in the short wave region of the visible spectrum it is a common error to disregard the lesser scattering and absorption of the long wave light. For example, tungsten-filament light contains short wave visible energy which suffers some scattering or absorption by fog as compared with sodium light. On the other hand it also contains long wave visible energy which suffers less scattering or absorption than sodium light does.

It has seemed desirable briefly to review previous investigations and to study the subject from the standpoint of relative visibility of sodium and tungsten-filament light sources. Luckiesh and Moss[9] made a study of the relative visibility of objects illuminated by sodium and tungsten light. They found that sodium light is superior to tungsten light in revealing detail of threshold size but that this advantage disappears for objects far above the threshold size, as are commonly encountered in everyday seeing and particularly on highways. They also found that the speed of seeing very small black objects on white background was greater for sodium than for tungsten light but that for large objects the speed of seeing was practically the same. They also revealed the disadvantage of sodium light due to the Purkinje effect at low levels of brightness such as may exist on highways at night. They studied other aspects of seeing but there still remained a question as to the penetration of fog. This we have investigated with a new procedure involving direct measurements of visibility of the light source.

The method of investigation consisted in placing a sodium lamp and a tungsten lamp in similar housings behind diffusing glasses of equal physical dimensions, brightness, and candlepower; and alternately measuring the relative visibilities of these two light sources during clear, hazy, slightly foggy, very foggy, misty, rainy and snowy weather. The light sources were about three feet apart in a window of the laboratory and were viewed from a distance of about 1000 feet across a wooded ravine.

TABLE II. *Relative visibilities of sodium and tungsten light sources, of 31 candlepower and of equal physical size and uniform brightness of 500 footlamberts, when observed in various kinds of weather at a distance of 1000 feet across a wooded ravine.*

Weather	Relative Visibility		Ratios of Tungsten Source to Sodium Source (Percent)
	Tungsten-Source	Sodium-Source	
1 Fairly clear	32.4	32.3	100.4
2 Moderate fog	18.2	18.7	97.2
3 Dense fog	11.1	11.2	99.1
4 Mist	24.5	24.9	98.4
5 Snowing	7.4	7.8	94.9

The light from the tungsten-filament lamp which we used in one pair of light sources had a color temperature of about 2800 degrees K. This was paired with sodium light produced by a standard sodium lamp now in practical use. This pair of lamps had luminous intensities of about 31 candles in the direction of the observers and a uniform brightness of 500 footlamberts over each six-inch circle. The low brightness pair of light sources was similar to the high brightness pair, excepting that each source was a circle 5 inches in diameter. They had luminous intensities of 4 candles in the direction of the observers and uniform brightnesses of 92 footlamberts. The tungsten light in this pair had a color temperature of about 2500 degrees K.

All measurements were made when the sun was obscured by clouds or fog or after sunset or dark. The relative visibilities were measured by twenty experienced observers using the Luckiesh-Moss visibility meter.[10] The standard method of observing was to expose one source to view and make 5 measurements; then eclipse this one and expose the other in quick succession. The average of 10 readings on each source constituted one observation. The number of observations varied from 32 to 90 for the various kinds of weather for the pair of sources of higher brightness and from 8 to 48 for the pair of lower brightness.

Measurements on both pairs of light sources

[9] M. Luckiesh and F. K. Moss, "Seeing in Tungsten, Mercury and Sodium Lights," Trans. I. E. S. **31**, 655 (1936). L. M. K. Boelter and F. A. Ryder, "Notes on the Behavior of a Beam of Light in Fog," Trans. I. E. S. **35**, 223 (1940). Gjon Mili, "Visibility of Signals through Fog," J. Opt. Soc. Am. **25**, 237 (1935).

[10] Matthew Luckiesh and Frank K. Moss, *The Science of Seeing* (D. Van Nostrand Company, New York, 1937).

TABLE III. *Ratio of relative visibilities of sodium and tungsten light sources, of 4 candlepower and of equal size and uniform brightness of 92 footlamberts, when observed in various kinds of weather at a distance of 1000 feet across a wooded ravine.*

WEATHER	RATIOS OF TUNGSTEN SOURCE TO SODIUM SOURCE (PERCENT)
Fairly clear	100.0
Moderate fog	99.7
Dense fog	99.5
Mist	98.1
Snowing	101.6

TABLE IV. *Ratio of visibilities of tungsten light to sodium light and compared with ratios of computed transmission factors of the atmosphere.*

WEATHER	RATIO OF OBSERVED VISIBILITIES		RATIO OF COMPUTED TRANSMISSION FACTORS
	31 C.P. 6 IN. LAMP	4 C.P. 5 IN. LAMP	
Clear	100.4	100.0	100.2
Hazy	97.2	99.7	98.5
Very humid	98.4	98.1	97.4
Very foggy	99.1	99.5	97.2
Light snow	94.9	—	97.6

were made during the four months of January, February, March and April, a period of considerable fog and cloudiness in the vicinity of Cleveland, Ohio. The visibility of each tungsten source is expressed as a percent of the visibility of the sodium source under like conditions. The results of the comparative measurements on the pair of high brightness sources are presented in Table II and the results on the pair of low brightness sources are presented in Table III. The probable errors in the data in the last columns are of the order of one to two percent.

It is apparent that the observed visibilities of the tungsten sources were practically equal to those of similar sodium sources under all atmospheric conditions which prevailed. By reference to Table II it may be seen that the average visibility of both sources through dense fog was only about one-third of what it was during clear weather. At times the fog was so dense that the low-brightness sources could not be seen and upon several other occasions they were barely visible. Although all measurements were made when the sun was obscured, it was observed that visibilities of both tungsten and sodium sources were higher during hours of darkness, but the ratio of their visibilities remained about the same at night as during the daytime. From an average of all measurements made during weather of low visibility it is found that on an average tungsten light was within 1.8 percent of that of sodium, whereas the average probable error was about 1.4 percent. This indicates that there is no significant difference between the visibilities of tungsten and sodium lamps of equal size and candlepower when seen at distances of about 1000 feet during ordinary foggy weather.

The relative transmissions of the earth's atmosphere during various kinds of weather for tungsten and sodium light were computed for several atmospheric conditions, using the relative spectral transmission values presented in Table I. The spectral distribution of energy from the tungsten source was assumed to be that of a blackbody at 2800 degrees K; and that from the sodium source to be entirely in the sodium lines at about $\lambda 5893$. The results of these computations are presented in the fourth column of Table IV from which it is seen that the ratios of the transmission factors of the atmosphere for tungsten and sodium light are about equal to the ratios of the visibilities of these sources in various kinds of weather at various hours of day and night.

It seems apparent from both the direct measurements of visibilities and the transmission factors of the atmosphere that the advantage of yellow light in foggy and misty atmospheres is greatly overrated and from a practical viewpoint is inappreciable if not entirely non-existent.

Zeeman Effects in the Palladium Spectrum

C. H. LINDSLEY AND N. ROSEN
Black Mountain College, Black Mountain, North Carolina

(Received May 16, 1941)

Zeeman data for 37 Pd I lines and 127 Pd II lines are given, based on measurements of Zeeman patterns photographed at M. I. T. in a magnetic field of about 87,500 gauss. g values for the energy levels arising from the $4d^9 5s$ and $4d^9 5p$ configurations of Pd I and the $4d^8 5s$ and $4d^8 5p$ configurations of Pd II are presented.

THE spectra of a large number of elements in a strong magnetic field have been photographed recently in the Spectroscopy Laboratories of the Massachusetts Institute of Technology. Professor George R. Harrison, who is in charge of this work, very kindly placed at our disposal the experimental data for palladium. Although the spectra of neutral[1] and singly ionized[2] palladium have previously been classified and the Zeeman effects measured, it nevertheless seemed worth while to analyze again the Zeeman patterns because of the increased accuracy made possible by the unusually high field strength.

TABLE I. *Zeeman effects of* Pd I *lines.*

Wave-length	Wave No.	Int.	Classification	g Values	
4473.590	22,347.16	60	$5s\,^1D_2 - 5p\,^3P^\circ_2$	1.040	1.484
4212.950 U	23,729.68	500	$5s\,^1D_2 - 5p\,^3F^\circ_2$	1.03	1.06
4169.842	23,974.99	200	$5s\,^3D_1 - 5p\,^3P^\circ_2$	0.496	1.479
4087.343	24,458.89	500	$5s\,^1D_2 - 5p\,^3P^\circ_1$	1.039	1.395
3958.642 U	25,254.07	500	$5s\,^1D_2 - 5p\,^3D^\circ_2$	1.036	0.987
3894.201	25,671.96	200	$5s\,^1D_2 - 5p\,^3D^\circ_3$	1.044	1.274
3832.291	26,086.68	150	$5s\,^3D_1 - 5p\,^3P^\circ_1$	0.500	1.398
3799.190	26,313.96	200	$5s\,^3D_2 - 5p\,^3P^\circ_2$	1.131	1.487
3718.909	26,881.99	300	$5s\,^3D_1 - 5p\,^3D^\circ_2$	0.499	0.987
3690.341	27,090.08	300	$5s\,^1D_2 - 5p\,^3F^\circ_2$	1.038	0.752
3634.695	27,504.81	2000	$5s\,^3D_3 - 5p\,^3P^\circ_2$	1.331	1.479
3609.548 U	27,696.43	1000	$5s\,^3D_2 - 5p\,^3F^\circ_3$	1.15	1.07
3571.155	27,994.18	40	$5s\,^3D_1 - 5p\,^3P^\circ_0$	0.496	0/0
3553.082 U	28,136.57	100	$5s\,^1D_2 - 5p\,^1F^\circ_3$	1.02	1.07
3516.943	28,425.69	1000	$5s\,^3D_2 - 5p\,^3P^\circ_1$	1.128	1.395
3489.772	28,647.00	150	$5s\,^1D_2 - 5p\,^3D^\circ_1$	1.044	0.835
3481.152	28,717.93	500	$5s\,^3D_1 - 5p\,^3F^\circ_2$	0.494	0.751
3460.774	28,887.03	300	$5s\,^3D_3 - 5p\,^3F^\circ_3$	1.333	1.063
3441.396 U	29,049.68	800	$5s\,^1D_2 - 5p\,^1D^\circ_2$	1.03	1.10
3433.449	29,116.92	1000	$5s\,^1D_2 - 5p\,^1P^\circ_1$	1.037	0.771
3421.24	29,220.8	2000	$5s\,^3D_2 - 5p\,^3D^\circ_2$	1.128	0.986
3404.580 U	29,363.80	2000	$5s\,^3D_3 - 5p\,^3F^\circ_4$	1.32?	1.22?
3373.001	29,638.71	800	$5s\,^3D_2 - 5p\,^3D^\circ_2$	1.135	1.278
3302.128	30,274.82	1000	$5s\,^3D_1 - 5p\,^3D^\circ_1$	0.497	0.824
3287.249	30,411.84	300	$5s\,^3D_3 - 5p\,^3D^\circ_2$	1.336	0.991
3258.780	30,677.51	300	$5s\,^3D_1 - 5p\,^1D^\circ_2$	0.500	1.112
3251.640	30,744.87	200	$5s\,^3D_1 - 5p\,^1P^\circ_1$	0.497	0.769
3242.703 U	30,829.60	2000	$5s\,^3D_3 - 5p\,^3D^\circ_3$	1.34	1.26
3218.974	31,056.86	300	$5s\,^3D_2 - 5p\,^3F^\circ_2$	1.129	0.753
3114.040 U	32,103.34	400	$5s\,^3D_2 - 5p\,^1F^\circ_3$	1.08	1.05
3065.306	32,613.72	10	$5s\,^3D_2 - 5p\,^3D^\circ_1$	1.126	0.837
3027.910 U	33,016.50	150	$5s\,^3D_2 - 5p\,^1D^\circ_2$	1.13	1.11
3021.749	33,083.81	2	$5s\,^3D_2 - 5p\,^1P^\circ_1$	1.118	0.764
3002.652	33,294.22	100	$5s\,^3D_3 - 5p\,^1F^\circ_3$	1.331	1.081
2922.492	34,207.39	200	$5s\,^3D_3 - 5p\,^1D^\circ_2$	1.335	1.115
2763.092	36,180.67	300	$a\,^1S_0 - 5p\,^3P^\circ_1$	0/0	1.397
2476.418	40,368.71	300	$a\,^1S_0 - 5p\,^3D^\circ_1$	0/0	0.831

The palladium spectrum was photographed from an arc of palladium and silver in the field of the large Bitter electromagnet[3] using the F, G, and H gratings described elsewhere.[4] The lines on the plates were then measured by means of the automatic comparator.[5] They lay in the range from about 2300 to about 4500Å.

TABLE II. Pd I *levels of* $4d^9\,5s$ *and* $4d^9\,5p$ *configurations.*

Level	Term Value Wave No.	Calc. g Value	Landé g Value	No. Meas.	No. Lines
$d^{10}\,^1S_0$	0.00	0/0	0/0	2	2
$5s\,^3D_3$	6,564.11	1.333	1.333	11	5
$5s\,^3D_2$	7,754.99	1.128	1.167	13	7
$5s\,^3D_1$	10,093.94	0.497	0.500	21	8
$5s\,^1D_2$	11,721.77	1.040	1.000	18	7
$5p\,^3P^\circ_2$	34,068.93	1.482	1.500	9	4
$5p\,^3F^\circ_3$	35,451.40	1.063	1.083	3	1
$5p\,^3F^\circ_4$	35,927.89	1.22?	1.250	1	1
$5p\,^3P^\circ_1$	36,180.64	1.396	1.500	8	4
$5p\,^3D^\circ_2$	36,975.93	0.988	1.167	9	4
$5p\,^3D^\circ_3$	37,393.71	1.276	1.333	4	2
$5p\,^3P^\circ_0$	38,088.11	0/0	0/0	2	1
$5p\,^3F^\circ_2$	38,811.86	0.752	0.667	6	3
$5p\,^1F^\circ_3$	39,858.33	1.081	1.000	2	1
$5p\,^3D^\circ_1$	40,368.73	0.831	0.500	7	4
$5p\,^1D^\circ_2$	40,771.46	1.114	1.000	5	2
$5p\,^1P^\circ_1$	40,838.80	0.768	1.000	7	3

TABLE III. *Comparison of g sums.*

Configuration	J Value	g (Calc.)	g (Landé)
$4d^9\,5s$	1	0.497	0.500
	2	2.168	2.167
	3	1.333	1.333
$4d^9\,5p$	1	2.995	3.000
	2	4.336	4.333
	3	3.420	3.417
	4	1.22?	1.250

[1] A. G. Shenstone, Phys. Rev. **36**, 669 (1930).
[2] A. G. Shenstone, Phys. Rev. **32**, 30 (1928); H. A. Blair, Phys. Rev. **36**, 173 (1930).
[3] G. R. Harrison and F. Bitter, Phys. Rev. **57**, 15 (1940).
[4] G. R. Harrison and J. R. McNally, Jr., Phys. Rev. **58**, 703 (1940).
[5] G. R. Harrison, J. Opt. Soc. Am. **25**, 169 (1935); Rev. Sci. Inst. **9**, 15 (1938); G. R. Harrison and J. P. Molnar, J. Opt. Soc. Am. **30**, 343 (1940).

TABLE IV. *Zeeman effects of* Pd II *lines.*

WAVE-LENGTH	WAVE NO.	INT.	CLASSIFICATION	g VALUES	
3738.86 U	26,738.5	15	$5s\ ^2G_{9/2}-ap\ ^4F^o_{7/2}$	1.09	1.09
3507.95	28,498.6	30	$5s\ ^2G_{7/2}-ap\ ^4F^o_{5/2}$	0.884	1.041
3468.54 U	28,822.4	50	$5s\ ^2G_{9/2}-ap\ ^2F^o_{7/2}$	1.13	1.13
3451.346 U	28,965.93	400	$5s\ ^4P_{5/2}-ap\ ^4D^o_{7/2}$	1.34	1.42
3272.56 U	30,548.3	60	$5s\ ^2D_{3/2}-ap\ ^4D^o_{3/2}$	1.18	1.15
3267.35	30,597.1	200	$5s\ ^4P_{3/2}-ap\ ^4D^o_{5/2}$	1.458	1.325
3243.131	30,825.54	60	$5s\ ^2F_{5/2}-ap\ ^4D^o_{7/2}$	(1.096)*	1.410
3210.448	31,139.34	60	$5s\ ^2G_{7/2}-ap\ ^2F^o_{5/2}$	0.890	1.113
3178.77	31,449.6	10	$5s\ ^2P_{3/2}-ap\ ^2D^o_{3/2}$	1.216	0.917
3170.26	31,534.1	50	$5s\ ^2D_{5/2}-ap\ ^2D^o_{5/2}$	1.240	1.021
3162.86	31,607.8	4	$5s\ ^2D_{3/2}-ap\ ^4D^o_{1/2}$	(1.165)*	0.035
3161.947	31,616.96	100	$5s\ ^4P_{1/2}-ap\ ^4D^o_{3/2}$	2.666	1.168
3155.59 U	31,680.7	40	$5s\ ^4P_{5/2}-ap\ ^4D^o_{5/2}$	1.32	1.32
3052.15	32,754.3	150	$5s\ ^4P_{3/2}-ap\ ^4D^o_{3/2}$	1.459	1.168
3050.084	32,776.48	100	$5s\ ^2D_{3/2}-ap\ ^4F^o_{3/2}$	1.163	0.722
3041.664	32,867.21	35	$5s\ ^2P_{1/2}-bp\ ^4P^o_{3/2}$	0.679	2.266
3032.20	32,969.8	100	$5s\ ^2F_{7/2}-ap\ ^4D^o_{7/2}$	1.147	1.405
2999.550	33,328.65	100	$5s\ ^4P_{5/2}-ap\ ^4G^o_{7/2}$	1.318	1.062
2980.655	33,539.91	200	$5s\ ^2F_{5/2}-ap\ ^4D^o_{5/2}$	1.095	1.329
2956.495	33,813.98	6	$5s\ ^4P_{3/2}-ap\ ^4D^o_{1/2}$	1.459	0.031
2954.394	33,838.03	60	$5s\ ^4P_{3/2}-ap\ ^4D^o_{3/2}$	1.333	1.185
2927.304	34,151.16	10	$5s\ ^2G_{7/2}-cp\ ^2F^o_{5/2}$	0.881	1.045
2893.089	34,555.03	100	$5s\ ^2D_{5/2}-ap\ ^2F^o_{5/2}$	1.238	1.117
2859.316	34,963.16	15	$5s\ ^4P_{5/2}-ap\ ^4F^o_{7/2}$	1.308	1.113
2857.726	34,982.61	100	$5s\ ^4P_{3/2}-ap\ ^4F^o_{3/2}$	1.462	0.722
2854.581 U	35,021.15	500	$5s\ ^2F_{7/2}-ap\ ^4G^o_{9/2}$	1.15	1.17
2846.762	35,117.33	15	$5s\ ^2P_{3/2}-cp\ ^2F^o_{5/2}$	1.191	1.047
2841.029 U	35,188.19	100	$5s\ ^2F_{5/2}-ap\ ^4G^o_{7/2}$	1.09	1.07
2839.892	35,202.28	100	$5s\ ^2G_{9/2}-cp\ ^2F^o_{7/2}$	1.098	1.250
2814.004	35,526.11	10	$5s\ ^2D_{3/2}-ap\ ^2D^o_{3/2}$	1.160	0.920
2802.473	35,672.28	10	$5s\ ^2P_{1/2}-cp\ ^2P^o_{1/2}$	0.67	1.07
2801.547	35,684.07	3	$5s\ ^2F_{7/2}-ap\ ^4D^o_{5/2}$	1.144	1.325
2796.606	35,747.11	5	$5s\ ^4P_{3/2}-ap\ ^4F^o_{5/2}$	(1.462)*	1.056
2779.701 U	35,964.50	5	$5s\ ^2P_{3/2}-cp\ ^2P^o_{1/2}$	1.23	1.13
2771.884	36,065.92	5	$5s\ ^4P_{5/2}-ap\ ^4F^o_{3/2}$	1.328	0.727
2742.603	36,450.95	100	$5s\ ^4P_{5/2}-ap\ ^2D^o_{5/2}$	1.325	1.022
2731.810	36,594.95	5	$5s\ ^4P_{1/2}-ap\ ^2D^o_{3/2}$	2.661	0.910
2727.891	36,647.53	200	$5s\ ^2F_{5/2}-ap\ ^4G^o_{5/2}$	1.096	0.714
2714.902 U	36,822.85	200	$5s\ ^2F_{5/2}-ap\ ^4F^o_{7/2}$	1.10	1.12
2714.319	36,830.76	150	$5s\ ^4P_{5/2}-ap\ ^4F^o_{5/2}$	1.319	1.048
2698.547	37,046.01	200	$5s\ ^4P_{5/2}-ap\ ^2F^o_{7/2}$	1.308	1.093
2688.551	37,183.73	200	$5s\ ^2D_{3/2}-bp\ ^4P^o_{3/2}$	1.172	1.319
2687.658	37,196.09	150	$5s\ ^2D_{3/2}-bp\ ^4P^o_{5/2}$	1.183	1.351
2684.761	37,236.22	100	$5s\ ^2D_{3/2}-bp\ ^4P^o_{1/2}$	1.166	2.271
2679.578 U	37,308.24	100	$5s\ ^2P_{3/2}-cp\ ^2P^o_{3/2}$	(1.220)*	1.177
2677.851 U	37,332.30	30	$5s\ ^2F_{7/2}-ap\ ^4G^o_{7/2}$	1.15	1.07
2661.143	37,566.68	100	$5s\ ^2D_{5/2}-cp\ ^2F^o_{5/2}$	1.238	1.065
2658.722 U	37,600.88	300	$5s\ ^2F_{7/2}-ap\ ^4F^o_{9/2}$	1.13	1.26
2657.563	37,617.28	200	$5s\ ^2P_{1/2}-cp\ ^2D^o_{3/2}$	0.684	1.186
2649.470	37,732.18	200	$5s\ ^4P_{3/2}-ap\ ^2D^o_{3/2}$	1.465	0.921
2642.168	37,836.45	100	$5s\ ^2G_{7/2}-bp\ ^4D^o_{5/2}$	0.888	1.233
2640.184	37,864.88	70	$5s\ ^2P_{1/2}-bp\ ^4D^o_{1/2}$	0.677	0.046
2637.069 U	37,909.60	100	$5s\ ^2P_{3/2}-cp\ ^2D^o_{3/2}$	1.20	1.20
2635.942	37,925.81	300	$5s\ ^2F_{5/2}-ap\ ^4F^o_{3/2}$	1.099	0.731
2628.254	38,036.74	200	$5s\ ^4P_{5/2}-ap\ ^2G^o_{7/2}$	1.303	0.994
2613.434	38,252.42	100	$5s\ ^4P_{1/2}-bp\ ^4P^o_{3/2}$	2.664	1.311
2609.862	38,304.77	200	$5s\ ^4P_{1/2}-bp\ ^4P^o_{1/2}$	2.661	2.259
2602.760 U	38,409.29	200	$5s\ ^2P_{3/2}-cp\ ^2D^o_{5/2}$	1.21	1.19
2595.969 U	38,509.76	150	$5s\ ^2D_{5/2}-cp\ ^2F^o_{7/2}$	1.24	1.26
2593.269	38,549.85	100	$5s\ ^2G_{9/2}-bp\ ^4D^o_{7/2}$	1.089	1.219
2584.132 U	38,686.15	75	$5s\ ^2P_{3/2}-bp\ ^4D^o_{3/2}$	1.18	1.18
2583.849 U	38,690.38	200	$5s\ ^4F_{5/2}-ap\ ^4F^o_{5/2}$	1.09	1.04
2577.097	38,791.70	150	$5s\ ^2F_{7/2}-ap\ ^4G^o_{5/2}$	1.154	0.726
2576.399 U	38,802.25	100	$5s\ ^2P_{3/2}-bp\ ^4D^o_{5/2}$	1.27	1.27
2575.490	38,815.95	100	$5s\ ^4P_{5/2}-ap\ ^2D^o_{3/2}$	1.327	0.918
2569.554 U	38,905.61	150	$5s\ ^2F_{5/2}-ap\ ^2F^o_{7/2}$	1.12	1.12
2565.507 U	38,966.98	200	$5s\ ^2F_{7/2}-ap\ ^4F^o_{7/2}$	1.14	1.02
2561.024	39,035.18	200	$5s\ ^4F_{5/2}-ap\ ^4D^o_{5/2}$	1.030	1.333
2551.848 U	39,175.54	100	$5s\ ^2G_{7/2}-kp\ ^2H^o_{9/2}$	0.90	0.91
2550.989	39,188.73	35	$5s\ ^2G_{7/2}-ep\ ^2D^o_{5/2}$	(0.886)*	1.187
2550.656 U	39,193.84	150	$5s\ ^2D_{3/2}-cp\ ^2F^o_{5/2}$	1.17	1.08
2544.833	39,283.52	200	$5s\ ^2G_{9/2}-kp\ ^2H^o_{9/2}$	1.111	0.915
2537.974	39,389.68	100	$5s\ ^4P_{3/2}-bp\ ^4P^o_{3/2}$	1.468	1.321
2537.169	39,402.18	100	$5s\ ^4P_{3/2}-bp\ ^4P^o_{5/2}$	1.462	1.346
2534.599	39,442.13	100	$5s\ ^4P_{3/2}-bp\ ^4P^o_{1/2}$	1.467	2.269
2514.478 U	39,757.72	200	$5s\ ^2D_{5/2}-cp\ ^2P^o_{3/2}$	1.24	1.14
2505.739 U	39,896.37	30	$5s\ ^2F_{5/2}-ap\ ^2G^o_{7/2}$	1.07	0.98
2498.784 U	40,007.41	150	$5s\ ^2F_{7/2}-ap\ ^2G^o_{9/2}$	1.14	1.15
2496.686 U	40,041.02	100	$5s\ ^2D_{3/2}-cp\ ^2P^o_{1/2}$	1.18	1.18
2489.611 U	40,154.80	75	$5s\ ^2P_{3/2}-ep\ ^2D^o_{5/2}$	1.18	1.18
2488.921 U	40,165.93	30	$5s\ ^4F_{9/2}-ap\ ^4D^o_{7/2}$	1.31	1.39
2488.412	40,174.15	10	$5s\ ^4F_{3/2}-ap\ ^4D^o_{5/2}$	0.409	1.155
2486.528 U	40,204.59	30	$5s\ ^4F_{7/2}-ap\ ^4G^o_{9/2}$	1.24	1.19
2477.005 U	40,359.14	25	$5s\ ^2D_{5/2}-cp\ ^2D^o_{3/2}$	1.29?	1.29?
2472.512	40,432.48	150	$5s\ ^2P_{1/2}-ep\ ^2D^o_{3/2}$	0.680	0.832
2471.152 U	40,454.73	150	$5s\ ^2F_{7/2}-ap\ ^2D^o_{5/2}$	1.14	1.04
2470.011 U	40,473.41	150	$5s\ ^4P_{5/2}-bp\ ^4P^o_{5/2}$	1.33	1.33
2469.254 U	40,485.82	150	$5s\ ^4P_{5/2}-bp\ ^4P^o_{3/2}$	1.32	1.32
2457.764 U	40,675.07	8	$5s\ ^2F_{5/2}-ap\ ^2D^o_{3/2}$	1.08	0.91
2457.260 U	40,683.42	10	$5s\ ^4F_{5/2}-ap\ ^4G^o_{7/2}$	1.03	1.06
2454.763	40,724.80	15	$5s\ ^2P_{3/2}-ep\ ^2D^o_{3/2}$	1.216	0.835
2448.164 U	40,834.56	100	$5s\ ^2F_{7/2}-ap\ ^4F^o_{5/2}$	1.18	1.08
2446.714 U	40,858.76	50	$5s\ ^2D_{5/2}-cp\ ^2D^o_{5/2}$	1.26	1.21
2446.182 U	40,867.65	100	$5s\ ^4F_{7/2}-ap\ ^4D^o_{5/2}$	1.22	1.35
2435.322 U	41,049.87	50	$5s\ ^2F_{7/2}-ap\ ^2F^o_{7/2}$	1.11	1.09
2433.104 U	41,087.29	50	$5s\ ^2G_{9/2}-kp\ ^2H^o_{11/2}$	1.08	1.09
2431.777	41,109.71	15	$5s\ ^4P_{1/2}-cp\ ^2P^o_{1/2}$	2.680	1.092
2430.929	41,124.05	30	$5s\ ^4F_{3/2}-ap\ ^4G^o_{5/2}$	0.440	0.718
2430.538	41,130.66	25	$5s\ ^2P_{1/2}-ep\ ^2S^o_{1/2}$	0.680	1.839
2426.868 U	41,192.86	50	$5s\ ^4F_{5/2}-ap\ ^4D^o_{3/2}$	1.03	1.18
2425.798	41,211.03	15	$5s\ ^2P_{1/2}-ep\ ^2P^o_{3/2}$	0.686	1.416
2424.480	41,233.42	100	$5s\ ^4F_{3/2}-ap\ ^4D^o_{1/2}$	0.423	0.046
2418.727 U	41,331.50	50	$5s\ ^2F_{5/2}-ap\ ^2F^o_{5/2}$	1.10	1.10
2415.614 U	41,384.34	30	$5s\ ^2D_{3/2}-cp\ ^2P^o_{3/2}$	1.14	1.14
2414.732	41,399.86	150	$5s\ ^4P_{3/2}-cp\ ^2F^o_{5/2}$	1.453	1.056
2408.736	41,502.92	100	$5s\ ^2P_{3/2}-ep\ ^2P^o_{3/2}$	1.227	1.406
2406.743 U	41,537.28	150	$5s\ ^2G_{9/2}-kp\ ^2F^o_{7/2}$	1.07	1.09
2388.289 U	41,858.21	40	$5s\ ^2D_{5/2}-bp\ ^4D^o_{7/2}$	1.26	1.26
2377.916	42,040.79	30	$5s\ ^2F_{7/2}-ap\ ^2G^o_{7/2}$	1.17	1.03
2372.154	42,142.90	50	$5s\ ^4F_{5/2}-ap\ ^4G^o_{5/2}$	1.031	0.714
2367.94	42,217.9	2	$5s\ ^4F_{9/2}-ap\ ^4G^o_{9/2}$	1.330	1.169
2362.322 U	42,318.28	35	$5s\ ^4F_{5/2}-ap\ ^4F^o_{7/2}$	1.03	1.11
2361.123	42,336.41	25	$5s\ ^2P_{1/2}-bp\ ^4S^o_{3/2}$	(0.681)*	0.893
2357.630	42,402.49	40	$5s\ ^4F_{3/2}-ap\ ^4F^o_{3/2}$	0.429	0.719
2354.797	42,453.50	25	$5s\ ^4P_{1/2}-cp\ ^2P^o_{3/2}$	2.672	1.130
2351.857 U	42,506.56	30	$5s\ ^2G_{7/2}-kp\ ^2F^o_{5/2}$	0.92?	0.92?
2351.338	42,515.94	60	$5s\ ^4F_{7/2}-ap\ ^4G^o_{7/2}$	1.248	1.075
2346.463	42,604.27	25	$5s\ ^2D_{5/2}-ep\ ^2D^o_{5/2}$	1.24	1.20
2337.77 U	42,762.7	25	$5s\ ^2D_{3/2}-bp\ ^4D^o_{3/2}$	1.16	1.16
2336.600 U	42,784.09	30	$5s\ ^4F_{7/2}-ap\ ^4F^o_{9/2}$	1.34	1.34
2336.411	42,787.55	30	$5s\ ^4F_{3/2}-ap\ ^2D^o_{5/2}$	0.419	1.016
2321.896	43,055.00	25	$5s\ ^4P_{1/2}-cp\ ^2D^o_{3/2}$	(2.666)*	1.178
2315.873	43,166.97	25	$5s\ ^4F_{3/2}-ap\ ^4F^o_{5/2}$	0.425	1.056
2308.604	43,302.87	30	$5s\ ^4P_{1/2}-bp\ ^4D^o_{1/2}$	2.671	0.051
2302.012 U	43,426.86	60	$5s\ ^4P_{3/2}-cp\ ^2F^o_{7/2}$	1.26	1.24
2299.432 U	43,475.58	25	$5s\ ^2F_{7/2}-ap\ ^2F^o_{5/2}$	1.19	1.19
2296.513 U	43,530.84	60	$5s\ ^4F_{9/2}-ap\ ^4G^o_{11/2}$	1.33	1.28

* Only the difference between the g values could be determined from the pattern. The g value in parentheses was taken from Table V and was used to determine the other g value.

The intensity of the magnetic field was determined from the Zeeman effects of the 3280 and 3382A lines of silver. It was found in this way that the field was 87,600 gauss. However, when the g values of the Pd I levels were calculated, it turned out that the g sums were all too high compared to the sums of the corresponding Landé g values. In order to obtain the best agreement between the two sets of sums the strength of the field was taken to be 87,470 gauss (a change of less than 0.2 percent). This change seemed justified in view of the fact that the silver lines were self-reversed, so that the Zeeman effects depended on the field in the cooler part of the arc which might be slightly different from that in the hotter part where most of the palladium lines were emitted.

The wave-lengths used and the intensities of the lines were taken from the *M. I. T. Wavelength Tables*.[6] In the cases of resolved patterns

[6] *M. I. T. Wavelength Tables* (John Wiley and Sons, New York, 1939).

TABLE V. Pd II *levels of $4d^8$ 5s configurations.*

LEVEL	TERM VALUE WAVE NO.	CALC. g VALUE	LANDÉ g VALUE	NO. LINES
$5s\ ^4F_{9/2}$	25,081.0	1.330	1.333	1
$5s\ ^4F_{7/2}$	27,094.3	1.248	1.238	1
$5s\ ^4F_{5/2}$	28,927.0	1.031	1.029	2
$5s\ ^4F_{3/2}$	29,945.6	0.424	0.400	4
$5s\ ^2F_{7/2}$	32,277.9	1.148	1.143	3
$5s\ ^2F_{5/2}$	34,422.0	1.096	0.857	4
$5s\ ^4P_{5/2}$	36,281.5	1.323	1.600	5
$5s\ ^4P_{3/2}$	37,365.0	1.462	1.733	9
$5s\ ^4P_{1/2}$	38,502.4	2.666	2.667	6
$5s\ ^2D_{3/2}$	39,571.1	1.165	0.800	4
$5s\ ^2D_{5/2}$	41,198.3	1.239	1.200	3
$5s\ ^2P_{3/2}$	43,647.8	1.220	1.333	3
$5s\ ^2P_{1/2}$	43,939.8	0.681	0.667	6
$5s\ ^2G_{9/2}$	44,505.7	1.099	1.111	3
$5s\ ^2G_{7/2}$	44,613.9	0.886	0.889	4

TABLE VI. *Comparison of g sums for $4d^8$ 5s.*

J VALUE	g (CALC.)	g (LANDÉ)
1/2	3.347	3.333
3/2	4.271	4.267
5/2	4.689	4.686
7/2	3.282	3.269
9/2	2.429	2.444

the g values were calculated in general to three places after the decimal, and the J values given in the classifications were verified from the Zeeman patterns. In the cases where the patterns were unresolved (indicated in the tables by U after the wave-length) the J values were assumed to be as in the classifications, and the g values were mostly computed to two places after the decimal. The plates contained a few lines involving configurations other than the ones in the tables, but the patterns were hazy and unresolved, so that it did not seem worth while to include them here.

NEUTRAL PALLADIUM

Table I gives the Zeeman data for 37 Pd I lines emitted in transitions from the $4d^9 5p$ configuration to the $4d^9 5s$ and $4d^{10}$ configurations. The g values are presented in the order of the terms in the classification. Table II contains the g values for the various levels of these configurations as determined from the data of Table I. Whenever it was possible, the values were obtained from resolved patterns only. The g values are probably correct to within ± 0.003 unit,

TABLE VII. Pd II *levels of $4d^8$ 5p configuration.*

LEVEL	TERM VALUE WAVE NO.	CALC. g VALUE	LANDÉ g VALUE	NO. LINES
$ap\ ^4D^\circ_{7/2}$	65,247.0	1.40	1.429	4
$ap\ ^4G^\circ_{9/2}$	67,299.0	1.17	1.172	4
$ap\ ^4D^\circ_{5/2}$	67,962.2	1.328	1.371	4
$ap\ ^4G^\circ_{11/2}$	68,611.5	1.28	1.273	1
$ap\ ^4G^\circ_{7/2}$	69,610.2	1.069	0.984	2
$ap\ ^4F^\circ_{9/2}$	69,878.4	1.28	1.333	2
$ap\ ^4D^\circ_{3/2}$	70,119.8	1.168	1.200	2
$ap\ ^4G^\circ_{5/2}$	71,069.5	0.718	0.571	4
$ap\ ^4D^\circ_{1/2}$	71,178.9	0.038	0.000	3
$ap\ ^4F^\circ_{7/2}$	71,244.7	1.11	1.238	4
$ap\ ^2G^\circ_{9/2}$	72,285.0	1.15	1.111	1
$ap\ ^4F^\circ_{3/2}$	72,348.0	0.724	0.400	5
$ap\ ^2D^\circ_{5/2}$	72,732.6	1.020	1.200	3
$ap\ ^4F^\circ_{5/2}$	73,112.4	1.047	1.029	4
$ap\ ^2F^\circ_{7/2}$	73,327.5	1.09	1.143	4
$ap\ ^2G^\circ_{7/2}$	74,318.7	0.99	0.889	3
$ap\ ^2D^\circ_{3/2}$	75,098.0	0.920	0.800	4
$ap\ ^2F^\circ_{5/2}$	75,753.6	1.115	0.857	2
$bp\ ^4P^\circ_{3/2}$	76,754.5	1.317	1.733	3
$bp\ ^4P^\circ_{5/2}$	76,767.4	1.34	1.600	3
$bp\ ^4P^\circ_{1/2}$	76,807.4	2.266	2.667	4
$cp\ ^2F^\circ_{5/2}$	78,765.3	1.056	0.857	3
$cp\ ^2P^\circ_{1/2}$	79,612.4	1.09	0.667	4
$cp\ ^2F^\circ_{7/2}$	79,708.0	1.25	1.143	3
$cp\ ^2P^\circ_{3/2}$	80,956.1	1.130	1.333	1
$cp\ ^2D^\circ_{3/2}$	81,557.2	1.186	0.800	1
$bp\ ^4D^\circ_{1/2}$	81,805.0	0.049	0.000	2
$cp\ ^2D^\circ_{5/2}$	82,057.0	1.20	1.200	2
$bp\ ^4D^\circ_{3/2}$	82,333.7	1.17	1.200	2
$bp\ ^4D^\circ_{5/2}$	82,450.0	1.233	1.371	1
$bp\ ^4D^\circ_{7/2}$	83,056.3	1.22	1.429	2
$kp\ ^2H^\circ_{9/2}$	83,789.7	0.91	0.909	2
$cp\ ^2D^\circ_{5/2}$	83,802.5	1.19	1.200	3
$cp\ ^2D^\circ_{3/2}$	84,372.3	0.834	0.800	2
$cp\ ^2S^\circ_{1/2}$	85,070.7	1.839	2.000	1
$cp\ ^2P^\circ_{3/2}$	85,151.0	1.411	1.333	2
$kp\ ^2H^\circ_{11/2}$	85,592.9	1.09	1.091	1
$kp\ ^2F^\circ_{7/2}$	86,043.1	1.09	1.143	1
$bp\ ^4S^\circ_{3/2}$	86,279.6	—	2.000	—
$kp\ ^2F^\circ_{5/2}$	87,120.4	0.92?	0.857	1
$cp\ ^2P^\circ_{1/2}$	88,038.1	—	0.667	—
$kp\ ^2G^\circ_{7/2}$	89,682.5	—	0.889	—
$kp\ ^2G^\circ_{9/2}$	89,982.4	—	1.111	—

Notation: ap denotes $4d^8(^3F)5p$; bp, $4d^8(^3P)5p$; cp, $4d^8(^1D;)5p$ ep, $4d^8(^3P)5p$; kp, $4d^8(^1G)5p$.

except in the case of $5p^3F^\circ_4$ where the g value had to be determined from a single unresolved, broad pattern. For comparison the Landé g values are included. It was found that by using the wave-lengths given in the *M. I. T. Wavelength Tables* more accurate term values than those found in the literature could be calculated; these new values are also given in Table II.

Table III gives a comparison of the g sums as calculated from the Zeeman data with the corresponding sums of the Landé g values. The agreement is quite good except in one case involving the uncertain g value already referred to.

Singly Ionized Palladium

There were a large number of Pd II lines on the plates, most of them representing transitions from the $4d^85p$ to the $4d^85s$ configurations; the Zeeman data for 127 of these are given in Table IV. Table V gives the g values for the lower group of levels, and Table VI the g sums. The g values for the upper group of levels are given in Table VII. Shenstone's notation for these levels is used because of its brevity; at the bottom of the table the corresponding parent terms of Pd III are indicated.[7]

The authors wish to thank Professor Harrison for the experimental data. They are also indebted to the North Carolina Academy of Sciences for a financial grant.

[7] R. F. Bacher and S. Goudsmit, *Atomic Energy States* (McGraw-Hill Book Company, Inc., New York, 1932).

AUGUST, 1941 J. O. S. A. VOLUME 31

The Lundegardh Flame Method of Spectrographic Analysis* †

VICTOR R. ELLS
The University of Missouri, Columbia, Missouri

(Received May 5, 1941)

THE various arc and spark techniques are practically the only methods used in quantitative spectrographic analysis in this country, the flame method developed by the Swedish botanist Henrik Lundegardh and his co-workers being for the most part neglected. Lundegardh has spent many years developing and improving the method, studying its application to the various elements, determining the most suitable lines and concentration ranges, and comparing the results obtained with those given by arc and spark methods.[1] The method has found favor in other European countries, particularly in England, where it has been used extensively for a number of years by several investigators including R. L. Mitchell at the Macauly Institute for Soil Research, Aberdeen, Scotland.[2] There are apparently but two places in this country where the method is being used, namely, Wellesley College, where it is being applied extensively in the analysis of various biological materials[3,4] and the University of Missouri.

The Lundegardh flame method is applicable to over thirty of the elements, these being listed, together with the most suitable lines and their sensitivity limits, in Table I. Most of the elements have but a very few flame lines, leading to comparatively simple spectra, even in complex mixtures. It is seen from the table that the alkali and alkaline earth metals, together with many of the minor elements regarded as important in plant and animal nutrition, are quite sensitive, being determinable in concentrations of one ten-thousandth molar or less. Hence the method is found to be very useful in the determination of these elements in soils, plant materials, animal tissues, etc. Furthermore, due to the exact control of conditions which is possible, the accuracy can readily be brought to within 5 percent of the amount present for most of the elements, and to within 2 percent or 3 percent for many.

The apparatus used is that manufactured by Adam Hilger and Company, and is sketched in Fig. 1. The materials to be analyzed are placed in solution, the solution is converted into a fine

* This paper is composed, in part, of material presented at the First and Second Midwest Spectrographic Conferences, held at the University of Chicago on March 30, 1940, and March 29, 1941.

† Contribution from the Department of Agricultural Chemistry, Missouri Agricultural Experiment Station, Journal Series No. 746.

[1] H. Lundegardh, *Die Quantitative Spectralanalyse der Elemente* (Jena, Verlag von Gustav Fischer), Part I, 1929; Part II, 1934.

[2] (a) R. L. Mitchell, J. Soc. Chem. Ind. **55**, 267 (1936); (b) R. L. Mitchell and I. M. Robertson, J. Soc. Chem. Ind. **55**, 269 (1936).

[3] M. A. Griggs, Science **89**, 134 (1939).

[4] M. A. Griggs, R. Johnstin and B. E. Elledge, Ind. Eng. Chem., Anal. Ed. **13**, 99 (1941).

spray by means of an atomizer and compressed air, the spray and air are mixed with acetylene, and the mixture is burned in front of the spectrograph slit. *A* is the air inlet and *F* the atomizer, which fits into the vessel *G* containing the solution through a ground glass joint. *B* is the inlet for the acetylene, which enters the glass burner tube through the silver nozzle *E*, where it mixes with the air and spray. A piece of blotting paper is placed at the bottom of the burner tube to absorb any solution condensing out on the walls and running down. The construction of the vessel *G*, however, insures that nearly all of the larger droplets will condense out there and run back into the solution at the bottom. This vessel fits into the side arm of the burner tube through another ground glass joint.

The burner tip *D* is placed 4–5 centimeters in front of the slit of the spectrograph (a Hilger medium quartz instrument, E498), and at such a height that the tip of the blue part of the flame is about 8–10 millimeters below the slit. The flame bands are considerably stronger closer to the blue tip. *C* is a nickel-chrome alloy mirror, which reflects the light going directly away from the slit and increases the intensity by about two-thirds. The slit width used is 0.04 millimeter.

The atomizer is shown in more detail in the lower part of Fig. 1. *A* is the entrance for the compressed air, *B* the inlet for the solution, and *C* the adjustable outlet (made of a platinum-iridium alloy, as is the burner tip *D*) for the air and spray. This may be screwed in and out to regulate the size of the opening through which the solution passes. The jet through which the air passes is about 0.3–0.4 millimeter in diameter.

The air pressure is controlled by means of a reducing valve on the compressed air tank. The acetylene pressure is controlled with another reducing valve, and in addition a water manometer is placed between the valve and the burner. The intensity of the emitted lines varies with the air and acetylene pressures; the first problem, then, in preparing to use the method is the finding of the most suitable pressures. For a given line of an element and a fixed acetylene pressure, an increase in the air pressure causes the intensity of the light emitted to pass through a flat maximum. As the acetylene pressure increases, this maximum is shifted to higher air pressures. One endeavors to choose the conditions which cause the flat maxima of the various elements being determined simultaneously to occur at as nearly the same pressures as possible, so that small variations will have little influence on the intensities. With the present equipment, the best pressures for determinations of mixtures of K, Na, Mn, Mg, Fe, Li, Sr and Ca are: air, two atmospheres; acetylene, twenty-two centimeters of water. These pressures are also quite suitable for the other metals which have been studied, although

TABLE I. *Lundegardh method. Elements, lines and sensitivities.*

Element	Line Wave-length	Sens. Limit in Milli-moles/Liter	Element	Line Wave-length	Sens. Limit in Milli-moles/Liter
Ag	3280.7	0.005	Na	5890.0/95.9	0.01
	3383.9	0.01		3302.3/02.9	0.5
Au	2676.0	0.1		2852.8/53.0	500
			Ni	3414.8	0.2
Ba	5535.5	1		3510.3	0.2
	4554.0	1		3515.1	0.2
				3524.5	0.2
Ca	4226.7	0.01		3493.0	0.4
				3002.5/03.6	10
Cd	3261.1	2			
			Pb	4057.8	0.6
Co	3526.9	0.2		3683.5	0.6
	4121.3	2		3639.6	0.6
	3044.0	4			
			Pd	3634.7	0.2
Cr	3578.7	0.1		3404.6	0.2
	3593.5	0.1			
	3605.3	0.1	Rb	4215.6	0.1
	4254.3	0.05		4201.8	0.1
	4274.8	0.1			
	4289.7	0.1	Ru	3786.0	0.1
				3725.9/28.0	0.1
Cs	4555.3	0.5			
	4593.2	1	Sr	4607.3	0.002
				4215.5	0.05
Cu	3247.5	0.01		4077.7	0.05
	3274.0	0.02			
			Tl	3775.7	0.002
Fe	3859.9	0.1		3519.2	0.1
	3719.9	0.1		5350.2	0.5
	3441.0	0.3		2767.9	2
Hg	2536.5	1	Zn	3072.1	500
K	4044.2/47.2	0.2	Other elements: dysprosium, gallium, gadolinium, indium, lanthanum, neodymium, praseodymium, rhodium, scandium, yttrium.		
	3446.4	2			
Li	6707.9	0.001			
Mg	2852.1	0.2			
Mn	4030.8	0.005			
	2798.3	0.5			

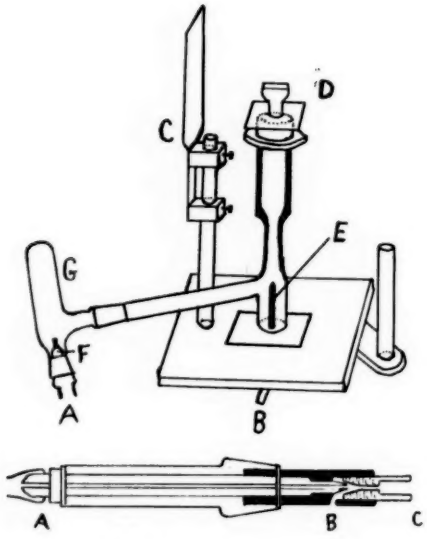

FIG. 1. (Above) Burner. *A*, to compressed air; *B*, to acetylene; *C*, mirror; *D*, burner tip; *E*, acetylene entrance nozzle; *F*, atomizer; *G*, vessel for solution. (Below) Atomizer. *A*, connection to compressed air tank; *B*, inlet for solutions; *C*, adjustable outlet for air and spray. (Reprinted from reference 5 [V. R. Ells and C. E. Marshall, Proc. Soil Sci. Soc. Am. **4**, 131 (1939)] by permission of the publishers.)

it is possible that somewhat better conditions could be found for certain of them. The flame produced is remarkably steady and constant, provided that drafts are excluded. If the amount of sodium present is small, it is practically as motionless in space as a still picture. Too much air cuts down the flame size and temperature; too much acetylene gives a more luminous flame and hence a stronger background.

The intensity also varies with the degree of atomization and the amount of solution getting into the flame, which vary with the viscosity and surface tension, and hence with the temperature and composition of the mixture. The atomizing process causes some cooling, making it desirable to wait a minute or more for equilibrium to be reached before making an exposure on a new solution. Within reasonable limits, variation in the amount of solution placed in the vessel *G* seems to have no appreciable effect. If the compositions are such as to affect markedly the viscosity and surface tension of the solutions, the offending substances may be added to the

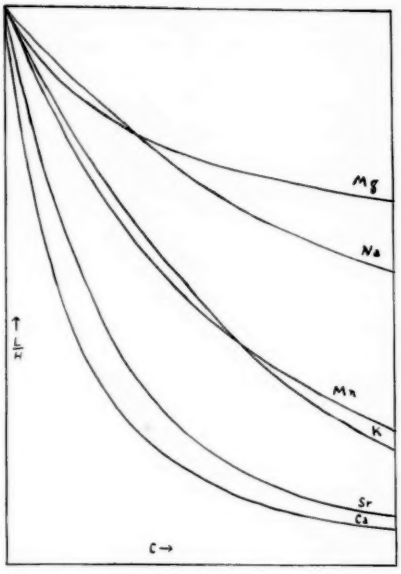

FIG. 2.

standard comparison solutions in like amounts, or internal standards may be used.

When changing from one sample to another, the atomizer, the vessel *G*, and the side arm of the burner tube are rinsed first with distilled water and then with some of the next sample. Several of the vessels (*G*) are available, so that after use they can be rinsed with distilled water and allowed to drain while the others are being used. Before disconnecting the ground glass joints for rinsing and introducing new solutions, the acetylene should be shut off to prevent the possibility of an explosion in the burner tube. Blanks are run in all cases to check the possibility of contamination from the chemicals used. Eastman 33 plates are usually used. However, S–C Ortho plates are used when sodium determinations using the yellow line are made, and Wratten and Wainwright Panchromatic plates are used for lithium determinations. Eastman developer D-19 and fixer F-5 are used, being freshly prepared at frequent intervals. After washing, the plates are given a final rinsing with distilled water.

We are using the method very extensively here in soil[5] and plant material analyses. For

[5] V. R. Ells and C. E. Marshall, Proc. Soil Sci. Soc. Am. **4**, 131 (1939).

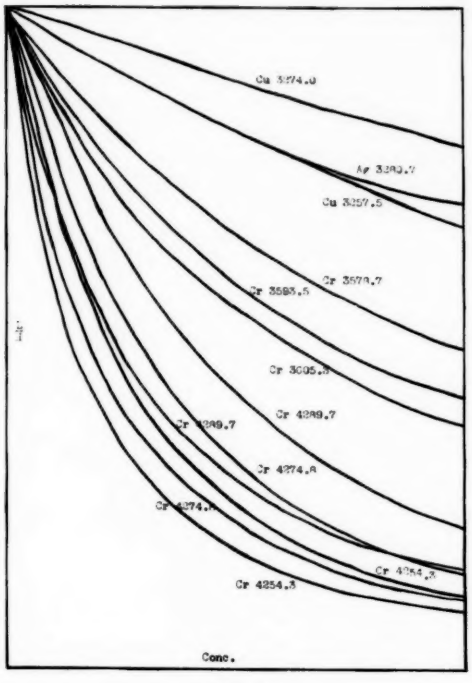

FIG. 3.

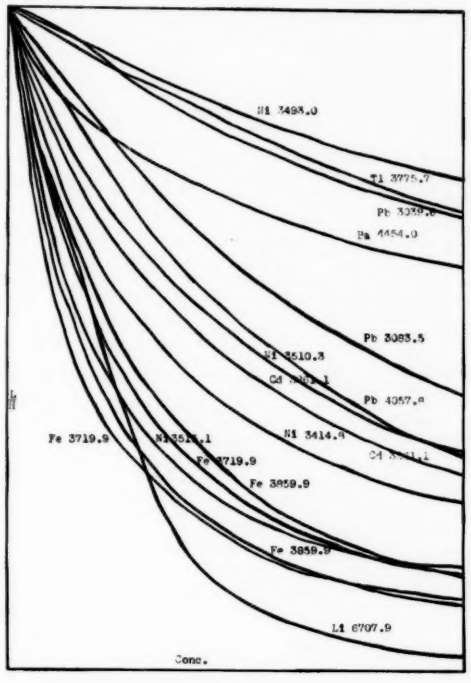

FIG. 4.

soils, 5–20 gram samples are selected, extracted, treated, and the solution brought to a volume of 50 cc. For plant materials, 0.2–0.5 gram of the dried substance is ashed, taken up in dilute hydrochloric acid, and diluted to 25 cc (considerably more concentrated solutions are necessary for the trace elements). Solutions prepared in these proportions are usually in a suitable state of concentration for direct determinations of K, Na, Mn, Mg and Sr, but must be diluted ten- to one-hundredfold for Ca determinations. Wet ashing methods are preferable to the dry heat process in the preparation of samples of organic material.

The plates are evaluated with a Leeds and Northrup recording microphotometer.[6] If I_0 is the incident intensity of the photometer light beam on the line, I_1 is the intensity of the radiation transmitted by the line, I_2 is the intensity of the radiation transmitted by the background, and I_3 is the intensity of the radiation transmitted by the line plus the background, then $\log I_0/I_1 = \log I_0/I_3 - \log I_0/I_2$, and it follows that the transmission of the line $= I_1/I_0 = I_3/I_2$. Since the continuous background is very uniform and invariant, its intensity being as characteristic a function as the line intensity, it may be used as an internal standard. The ratio of the distance $L(=aI_3)$ from the opaque plate zero point to the line maximum to the distance $II(=bI_2)$ to a point in the background at a given distance from the center of the line is determined. This ratio varies from 0 to 1 as the concentration decreases, and is plotted against the concentration for a series of five standard solutions, giving curves as in Figs. 2, 3 and 4, which are effectively transmission curves for the lines on the plate. From the L/II values obtained from the unknown solutions, the corresponding concentrations are read off. For most of the elements a twenty-fold concentration range may be employed for the standard solutions. The standards are photographed on each plate, and one of them may be

[6] Described by R. C. Machler, *Proceedings of Seventh Summer Conference on Spectroscopy and Its Applications* (John Wiley and Sons, New York, 1940), p. 65.

repeated at intervals to check for any variations in characteristics on various parts of the plate. The slit height used is 1½ mm, so that 35 spectra may be placed upon each plate. Both standards and samples are photographed in duplicate or triplicate and average values taken. The best exposure time under the conditions used seems to be about one minute. Decreasing the slit width decreases the intensity of the background on the plate to a greater extent than that of the lines, which may be made use of to cut down excessive background intensity. However, when a microphotometer is to be used, one must be careful not to narrow the slit too much.

Tables II and III show the results obtained with various elements in solutions of known concentrations. Table IV shows the concentrations of the metals used in the standards to cover the most suitable range. Tables V and VI indicate results obtained in potassium and iron analyses, respectively, comparing values obtained by the chemical and spectrographic methods, and those obtained spectrographically using different lines. The agreement is good in practically all cases.

TABLE II. *Results with known solutions.* (*Concentrations in millimoles per liter.*)

Li 6707.9A. Known conc.	0.209	0.093	0.039	0.020
Determination 1.	.216	.095	.036	.018
2.	.215	.090	.037	.019
3.	.206	.088	.040	.019
Average	.212	.091	.038	.019
K 4044.2A. Known conc.	3.35	1.40	0.777	0.198
Determination 1.	3.26	1.41	.75	.23
2.	3.31	1.46	.73	.19
3.	3.34	1.48	.74	.20
Average	3.30	1.45	.74	.21
Mn 4030.8A. Known conc.	0.126	0.047	0.019	0.010
Determination 1.	.122	.043	.018	.010
2.	.123	.043	.019	.010
3.	.123	.045	.019	.010
Average	.123	.044	.019	.010
Sr 4607.3A. Known conc.	0.042	0.019	0.0100	0.0050
Determination 1.	.041	.018	.0100	.0048
2.	.039	.017	.0100	.0040
3.	.037	.013	.0099	.0039
Average	.039	.016	.0100	.0042
Ca 4226.7A. Known conc.	0.167	0.056	0.029	0.010
Determination 1.	.143	.055	.027	.0095
2.	.159	.056	.028	.010
3.	.157	.058	.029	.010
Average	.153	.056	.028	.010
Mg 2852.1A. Known conc.	2.51	0.93	0.582	0.198
Determination 1.	2.44	.88	.55	.22
2.	2.76	.97	.54	.18
3.	2.44	.98	.57	.15
Average	2.55	.94	.55	.18
Na 3302.3A. Known conc.	4.19	1.86	0.388	
Determination 1.	4.06	2.00	.54	
2.	4.10	2.00	.51	
3.	4.10	2.07	.52	
Average	4.09	2.02	.52	

In Table VII are indicated the magnitudes of the errors which may be introduced by variations in the air and acetylene pressures and the time of exposure from the normal values of two atmospheres, twenty-two cm of water, and one minute, respectively. These variations were purposely chosen to be considerably larger than any possible experimental errors. The pressures are quite steady and can be accurately and readily readjusted if they should vary. The maximum deviations in actual determinations in air and acetylene pressures are 0.05 atmosphere and 0.3–0.4 cm, respectively, and the exposure times can be controlled to within 0.4 second. Experimental errors from these sources are thus seen to be quite small.

Another advantage of this method is the comparative lack of interactions between various cations, and between cations and anions, which affect the intensities of the emitted lines. However, there are a few things which must be watched for. The presence of aluminum in concentrations greater than one milligram per liter depresses the intensities of the calcium and strontium lines. This effect is quantitative, and Mitchell[2b] has made use of it to determine aluminum in amounts ranging from two to ten milligrams per liter. For the determination of calcium in the presence of aluminum, one can work at greater dilutions and add a little strontium; for strontium determinations, calcium may be added. Also one may add like amounts of aluminum to the standards, or go through the procedure for removing sesquioxides. Aluminum usually gives trouble only in hydrochloric acid extracts.

High acid concentrations result in low values in the determination of some of the elements, particularly potassium, calcium and strontium. Other elements show smaller effects. Results for magnesium tend to be somewhat high in strongly acid solutions. Table VIII shows the acid effect.

TABLE III. *Results with known solutions. (Concentrations in millimoles per liter.)*

Cr Known	0.111	0.222	0.286	0.67	1.11	1.43	0.118	0.194	0.333
3605.3	.111	.201	.268	.68	1.25	1.45			
3593.5	.101	.225	.291	.69	1.18	1.43			
3578.7	.100	.226	.294	.70	1.25	1.51			
4289.7	.106	.235	.295	.70	1.20	1.54	.120	.187	.355
4274.8	.114	.225	.294	.73	1.21	1.53	.120	.186	.322
4254.3	.108	.228	.294	.70	1.24	1.52	.114	.187	.329
Cu Known	0.016	0.033	0.043	0.100	0.167	0.214			
3274.0	—	.030	.043	.103	.171	.210			
3247.5	.014	.031	.045	.105	.171	.215			
Cd Known	28.57	13.33	23.26	6.67	3.88	2.36			
3261.1	28.48	13.83	23.08	6.44	3.93	2.44			
Pb Known	0.67	1.33	1.71	4.00	6.67	8.57			
4057.8	.66	1.28	1.47	3.94	6.72	8.54			
3083.5	.68	1.20	1.55	4.01	6.67	8.10			
3039.6	.60	1.20	1.49	3.94	6.58	8.34			
Ni Known	2.86	2.33	1.33	0.667	0.388	0.236			
3510.3	2.71	2.29	1.29	.61	.37	.20			
3414.8	2.56	2.31	1.27	.61	.36	.20			
3515.1	2.48	2.07	1.25	.60	.36	.21			
3493.0	2.46	2.14	1.34	.63	.37	—			
Tl Known	0.0286	0.0133	0.0233	0.00667					
3775.7	.0282	.0140	.0232	.00663					
Ag Known	0.0714	0.0333	0.0581	0.0167	0.0097				
3280.7	.0694	.0322	.0554	.0160	.0100				

TABLE IV. *Concentrations in millimoles per liter of standard solutions to cover the suitable range.*

ELEMENT		×1	×2	×5	×10	×20
Ca	4226.7	0.25	0.125	0.05	0.025	0.0125
Ag	3383.9	0.10	0.05	0.02	0.01	0.005
Ba	4554.0	20	10	4	2	1
Cd	3261.1	40	20	8	4	2
Cr	4254.3	2	1	0.4	0.2	0.1
Cu	3247.5	0.10	0.05	0.02	0.01	0.005
	3274.0	0.30	0.15	0.06	0.03	0.015
Fe	3719.9	5	2.5	1	0.5	0.25
K	4044.2	5	2.5	1	0.5	0.25
Li	6707.9	0.25	0.125	0.05	0.025	0.0125
Mg	2852.1	5	2.5	1	0.5	0.25
Mn	4030.8	0.25	0.125	0.05	0.025	0.0125
Na	3302.3	10	5	2	1	0.5
	5890.0	0.2	0.1	0.04	0.02	0.01
Ni	3414.8	4	2	0.8	0.4	0.2
Pb	3683.5	12	6	2.4	1.2	0.6
Sr	4607.3	0.10	0.05	0.02	0.01	0.005
Tl	3775.7	0.04	0.02	0.008	0.004	0.002

TABLE V. *Results with potassium compared with results by a chemical method. (Solutions of plant ash in percent.)*

CHEM.	SPEC.	CHEM.	SPEC.
1.99	2.01	2.24	1.95
1.67	1.87	2.60	2.53
1.93	1.97	2.30	2.41
2.00	1.95	2.63	2.49
0.90	0.81	2.04	2.04
0.90	0.75	1.32	1.26
1.29	1.19	2.89	2.95

TABLE VI. *Results in percent, samples ashed and analyzed for iron, using two lines.*

SAMPLE	3860A	3720A
1–1	0.0370	0.0377
1–2	.0354	.0348
2–1	.0486	.0490
2–2	.0483	.0461

TABLE VII.

	Effects of Variation of Acetylene Pressure			Effects of Variation of Air Pressure		
	22 cm	23 cm	21 cm	2.00 Atmos.	1.75 Atmos.	2.25 Atmos.
K	1.00	0.96	1.03	1.00	0.85	1.10
	5.00	4.96	5.22	5.00	4.25	5.22
	2.50	2.52	2.77	2.50	2.66	3.10
	0.50	0.52	0.55			
Mn	0.025	0.027	0.030	0.050	0.044	0.059
	.050	.052	.055	.125	.124	.151
	.125	.123	.135	.250	.204	.271
	.250	.254	.268			
Ca	0.025	0.027	0.025	0.125	0.148	0.131
	.050	.053	.050	.050	.047	.044
	.125	.131	.128			
Sr	0.0100	0.0105	0.0105	0.0200	0.0184	0.0182
	.0200	.0208	.0203	.0500	.0590	.0516
	.0500	.0530	.0516			
Na	1.00	0.95	1.02	2.00	1.60	2.51
	2.00	1.88	2.28	5.00	4.82	6.64
	5.00	4.70	5.41			
	10.00	10.43	11.51			
Mg	0.50	0.51	0.65	1.00	0.63	1.34
	1.00	1.06	1.26	2.50	1.93	3.38
	2.50	2.32	2.89	5.00	2.59	5.70
	5.00	4.46	6.55			

Effects of Variations in Exposure Time

Exp. (sec.)	K			Mn			Na		
60	conc. 2.50	1.00	5.00	0.125	0.050	0.250	5.00	2.00	10.00
55	2.23	.81	4.33	.112	.045	.214	4.46	1.60	8.23
58	2.42	.94	4.60	.121	.048	.232	4.68	1.78	8.89
59			4.79			.232			9.63
61			5.07			.255			10.35
62	2.64	1.06	5.30	.133	.052	.269	5.28	2.11	10.47
65	3.06	1.09	5.94	.149	.054	.285	6.05	2.20	12.25

	Ca		Sr		Mg	
60	conc. 0.125	0.050	0.0500	0.0200	2.50	1.00
55	.113	.044	.0447	.0176	1.83	0.82
58	.119	.048	.0473	.0190	2.09	0.97
62	.132	.053	.0527	.0212	2.64	1.05
65	.141	.056	.0577	.0226	3.20	1.17

If the standards and unknown solutions are in the range 0–0.2 normal in acid, the errors introduced by differences in acidity between standards and unknowns are small. For protection of the metal parts of the apparatus, and to minimize the solution of elements from the glass containers, the solutions are kept below 0.1*N* in acid content if possible. If unknowns have an acid content greater than 0.2*N*, like amounts of acid are added to the standards.

Sodium may affect potassium determinations, tending to give low results, but only at high concentrations, where the sodium is seventy-five times, or more, greater in amount than the potassium. Sodium chloride may be added to the standards to eliminate any discrepancy in such cases, as the analysis of sea water, etc. High concentrations of sodium and magnesium give a general blackening of the background, which tends to give low results for the other elements unless compensated for by addition of similar amounts of sodium and magnesium to the standards. In Table IX are shown results obtained with prepared solutions, illustrating the effect of high sodium concentrations. The addition of sodium to the standards in proper amount is seen to produce accurate determinations.

Organic compounds in the solutions also give

rise to a general blackening of the background, and error may be avoided by addition of like amounts of pure organic material to the standards. An example is the analysis of sugar solutions, syrups, etc. Lundegardh[1] states that milk may be tested directly without great error.

Usually it is sufficient to use the procedures described above, but occasionally it may be desired to make use of internal standards. Lundegardh recommends copper for sugar solutions, and cobalt or chromium for milk. This technique may be best for solutions containing fat globules, proteins, etc., and with those containing small solid particles which affect the atomizer action. The same amount of internal standard is added to all the samples, but it is allowed to vary in the standards in the same ratio as the other elements. The concentrations of internal standard in the samples are determined from the standard curve and any correction necessary is applied to all the readings made on the samples. For example, if two millimoles per liter of internal standard were added to the samples, and the values for the concentration obtained from the standard curve are 1.8, all of the values for the different elements are multiplied by the ratio 2/1.8.

Some trouble was incurred, in using soft glass and new Pyrex bottles for storage of the sample solutions, by the solution of sodium, and in some cases potassium, from the glass surfaces. It was found to be safest to keep solutions in which sodium and potassium are to be determined only in aged Pyrex containers.

TABLE VIII. *Effect of acid concentration of solutions.*

ELEMENT	Fe	Na	Mn	Mg	Sr	Ca	K
			Standard 0.1 Normal				
Conc.	1.25	2.50	0.0625	1.25	0.0250	0.0625	1.25
Normality							
0.2	1.24	2.41	0.0607	1.34	0.0234	0.0588	1.19
0.5	1.21	2.37	.0580	1.39	.0207	.0521	1.09
1	1.19	2.17	.0585	1.34	.0177	.0471	1.01
3	1.30	2.09	.0594	1.48	.0122	.0337	0.76
Conc.		2.86		1.43	0.0286	0.0704	1.43
0.1		2.88		1.46	.0306	.0709	1.42
0.05		2.95		1.37	.0311		1.48
0.01		2.94		1.45	.0311		1.47
Neut.		3.04		1.57	.0323		1.48
			Neutral Standard				
Conc.			0.0704	2.50	0.0286	0.0704	1.43
0.1			.0650	2.39	.0273	.0695	1.36
0.05			.0693		.0275		1.43
0.01			.0700		.0280		1.41
Neut.			.0710		.0290	.0714	1.43

TABLE IX. *Studies involving high sodium concentrations. (Concentrations in millimoles per liter.)*

ELEMENT	SOLUTIONS, 0.5*M* NaCl KNOWN CONC.	RESULTS WITH VARIOUS STANDARD SOLUTIONS NORMAL	WITH 1*M* NaCl	WITH 0.5*M* NaCl
K	3.50	2.61	4.46	3.54
K	2.50	1.85	3.22	2.47
K	3.75	2.84	4.59	3.71
Mn	.0200	.0163	.0233	.0202
Mn	.0170	.0130	.0210	.0163
Mn	.0150	.0114	.0214	.0160
Ca	.1250	.073	.171	.122
Sr	.0500	.0308	.0684	.0515
Sr	.0035	.0027	.0047	.0034
Fe	2.50	2.11	3.06	2.41

The anions, chloride, bromide, iodide, sulphate, and possibly others, can be determined by indirect methods. The halides are precipitated by silver nitrate in a solution of known concentration, and the resulting decrease in silver concentration is noted after filtration. Sulphate is determined similarly, using strontium chloride.

The spectral region 3250A–4600A is the most favorable in the flame method, and fortunately the great majority of the lines used fall there. The background is very uniform and homogeneous over the whole range. Strong bands occur from 3050A–3200A which interfere with zinc determinations. There are weak bands beyond 3050A to shorter wave-lengths, but these do not cause much interference. The magnesium line (2852A), for example, falls in this region, but no difficulty is experienced in its measurement.

A series of eight or nine solutions in triplicate, or twelve or thirteen in duplicate, together with standards, may be photographed on a plate in two to two and one-half hours. The time taken for the microphotometering and subsequent calculations depends, of course, upon the number of elements being determined in the given samples. Five elements may be determined in a series of samples in an average time of forty minutes per sample, or eight minutes per element. The time taken to determine any

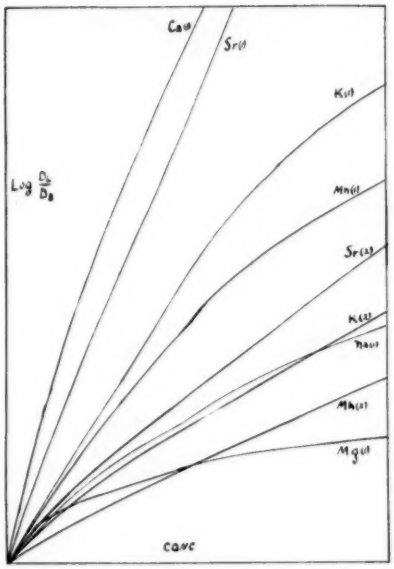

FIG. 5.

element or elements for which the solution must be diluted is necessarily greater.

TABLE X.

L / H	LOG $\frac{D_L}{D_B}$	L / H	LOG $\frac{D_L}{D_B}$	L / H	LOG $\frac{D_L}{D_B}$
K		Mn		Mg	
3.20	3.18	0.1410	0.1390	1.34	1.34
1.41	1.37	.0412	.0428	1.48	1.50
3.36	3.30	.0222	.0228	1.34	1.36
1.48	1.47	.0837	.0821	1.39	1.38
0.64	0.66	.0274	.0279	0.25	0.26
3.93	3.89	.0821	.0796	0.50	0.49
1.01	1.01	.0585	.0593	1.03	1.00
0.76	0.76	.0594	.0579	2.25	2.40
1.19	1.22	.0607	.0603		
1.09	1.10	.0580	.0579		
0.48	0.46	.0125	.0133		
0.94	0.95	.0246	.0230		
2.23	2.26	.0456	.0456		
		.1125	.1116		
Ca		Sr		Na	
0.0471	0.0475	0.0177	0.0182	2.17	2.18
.0337	.0343	.0122	.0122	2.09	2.02
.0588	.0580	.0234	.0234	2.41	2.24
.0521	.0524	.0207	.0209	2.37	2.30
.0222	.0222	.0099	.0096	0.50	0.60
.0456	.0458	.0191	.0196	0.87	1.00
.1044	.1047	.0460	.0454	1.82	1.76
				4.42	4.60

Recording paper for the microphotometer graduated in density values has recently become available. Density values for the line and background are read off directly and subtracted, giving the log intensity ratio (multiplied by plate gamma) usually plotted against concentration in arc and spark analysis. This ratio is designated as D_L/D_B in Fig. 5, where examples of the curves obtained are given (for two plates, designated as 1 and 2, having different characteristics. Both are Eastman 33 plates, but are from different consignments). D_L=deflection of line from clear plate zero point; density of line equals log D_L, etc. Log $D_L/D_B=\gamma \log I_L/I_B$, where the I's are intensities. The results obtained by this method of computation agree with those obtained from the transparency plot, as shown by Table X, and a considerable saving of time is effected.

The present writer has obtained very successful results with the Lundegardh flame method and in much less time than with arc and spark methods. Since the method is more rapid than arc and spark methods and gives more accurate results with less painstaking procedures, it is to be recommended for those metals to which it is applicable in samples available in sufficiently large quantities to give a large enough concentration in the solutions prepared from them. Very small amounts of samples suffice for the more abundant elements, but larger samples are required for the trace elements. Only a few cubic centimeters of solution are needed; when the apparatus is clean and dry, requiring no rinsing, as little as 2–3 cc will suffice. The conditions are readily controllable and variations in pressures, etc., can easily be kept very small. A good mechanic should be able to construct the apparatus for using the method quite inexpensively, as compared to the price of the purchased outfit. Less resistant (and less expensive) alloys may be used for the metal parts, provided that provisions are made for replacing them when necessary.

A Supersonic Cell Fluorometer

H. B. BRIGGS
Bell Telephone Laboratories, New York, New York

(Received April 26, 1941)

A method is described for the measurement of the rise and decay of luminescence in phosphors excited by cathode-ray beams. It is particularly suited to the investigation of phosphors classed as fast, i.e., those in which major changes in intensity occur in a few microseconds. The method is based on the use of a supersonic cell arranged to produce the Debye-Sears diffraction effect. High speed shutter action is obtained by modulating the supersonic wave train to produce short steep-sided pulses. Light intensities sufficient for direct measurement in terms of photoelectric cell response are obtained by synchronizing the periodic excitation of the phosphor with the diffracting wave pulses in the liquid. Time intervals in the decay process are measured in terms of distances traversed by the sound waves in water. Several methods of using the device are described, and some results obtained by these methods are shown.

A SUPERSONIC cell arranged to produce the Debye-Sears diffraction effect[1] may readily be adapted to the measurement of the rise and decay of luminescence in phosphors excited by cathode rays. The method to be described here has been used by the author during the past year, and has been found particularly suited to measurements on fast phosphors, where the excitation and decay times are of the order of a few microseconds. The elements of this measuring system consist of (1) a high speed shutter which passes light from the emitting phosphor to the recording device, (2) a device for synchronizing the shutter with the periodic excitation of the phosphor so that the same time interval in each excitation cycle is selected and (3) provision for introducing a variable time delay between the shutter opening and the phosphor excitation in order to allow successive intervals of the decay process to be recorded. The manner in which these are accomplished is most easily described after reference to a diagram of the apparatus.

APPARATUS

In Fig. 1, SS' represents the optical system of a spectrometer in which the supersonic cell replaces the usual diffraction grating, and a photoelectric cell replaces the eye. Light from the fluorescent screen T illuminates the collimator slit S, is rendered parallel by the lens L_1, and passes through the supersonic cell C, where it is diffracted by the sound waves generated by the oscillating quartz crystal Q. The diffraction pattern consisting of several orders is formed in the focal plane of L_2. An opaque bar stop S' of sufficient width to block out the zero order is placed in this plane. The diffracted light passes on either side of this stop to reach the photoelectric cell P whose response is measured with the quadrant electrometer E.

The operation of the system as shown in Fig. 1 may be described briefly as follows. A rectangular wave of voltage of known repetition frequency is applied simultaneously to both the grid of the cathode-ray tube and the grid of the modulator tube of the modulator oscillator unit. At the cathode-ray tube a beam of electrons flows for the duration of the pulse, giving rise to a screen excitation cycle. At the same time the quartz crystal is excited and gives rise to a short pulse of high frequency supersonic waves.

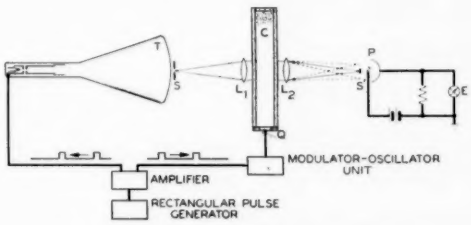

FIG. 1. Schematic diagram of the supersonic cell fluorometer.

[1] P. Debye and F. W. Sears, Proc. Nat. Acad. Sci. Wash. **18**, 410 (1932).

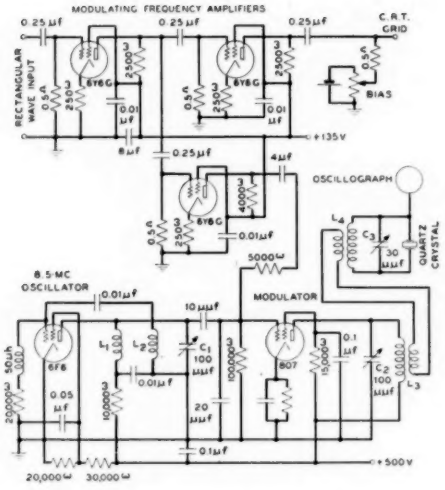

FIG. 2. Circuit diagram of the modulating frequency amplifiers and the modulator oscillator unit.

This pulse advances through the liquid at a known velocity and diffracts the light as it passes through the light beam in the cell. It follows that the diffracted light is that emitted by the screen at a definite measurable time interval after the screen was excited. The phenomenon repeats cyclically, so that succeeding wave pulses diffract light from exactly the same interval of each screen excitation cycle. Succeeding intervals in the excitation cycle are obtained by shifting the position of the supersonic cell to increase the distance between the quartz crystal and the light beam in the cell.

A supersonic cell suitable for this work presents little difficulty in construction. The one in use has a rectangular cross section, the inside dimensions being $1\frac{1}{2}$ in. by $1\frac{1}{2}$ in. The over-all length is 12 inches. Top and bottom are of $\frac{1}{4}$-in. sheet brass, accurately milled to a uniform width. The sides are of selected plate glass 2 in. by $\frac{1}{4}$ in. by 12 inches cemented to the brass. The primary requirement in the windows is that the slit image shall not be deviated or distorted by them in an amount sufficient to allow undiffracted light to pass the bar stop S' as the cell is moved across the light beam. Scattering of the light due to flaws, scratches or other causes is also to be avoided. One end of the cell is closed by the quartz crystal and its mounting. The brass base is curved upward to close the opposite end. A portion of the top is left open for filling the cell and inserting a plug of glass wool to prevent reflection of the sound waves back through the liquid. The cell is attached to a bevelled base which slides over a track attached to the prism table of the spectrometer. Displacements in a direction perpendicular to the light beam are read by an index and scale attached to the base and track respectively.

A piezoelectric quartz plate 25 by 25 by 0.33 mm, having a fundamental vibration frequency of 8.5 megacycles, was used to produce the supersonic waves. The electrodes were of gold, sputtered to form a conducting layer on each side of the quartz plate. The edges of the plate were shielded during the sputtering to provide insulation between the two electrodes. The quartz plate was mounted so that one face was in contact with the liquid and the other face was open to the air. Due to the low acoustical impedance of the air this method of mounting allows efficient use of the vibrational energy of the crystal.

Water was used in the cell because of its low absorption coefficient. The high velocity of propagation of the sound waves in water gave a good distance to time ratio, i.e., 1 cm = 6.67 μsec., but the coarser grating effect due to this high velocity resulted in a lower light handling power for the cell.

For convenience in adjustment the cell was mounted on the prism table of a small Gaertner spectrometer. The low light gathering power of the F9 optical system of this spectrometer, while adequate for most of the measurements tried, imposed an unnecessary restriction on the range of intensities which could be investigated.

A potassium hydride photoelectric cell was used in obtaining the results shown in Figs. 4 to 7, inclusive. The results in Fig. 8 were obtained using a caesium-antimony photoelectric cell. Both are strongly blue sensitive cells and the response obtained must be considered with respect to the color sensitivity of the cell.

CIRCUITS AND ADJUSTMENTS

Details of the circuits used in this work are shown in Fig. 2. In addition to these a rec-

tangular wave generator and television sweep circuits were available.

The arrangement shown in the figure was used with a stationary unfocused spot on the cathode-ray tube screen. The rectangular wave generator output was amplified through two stages and fed to the grid of the cathode-ray tube to produce the beam current pulses. The biasing arrangement shown gave a ready control of the beam current intensity. The details of construction of the 8.5-megacycle oscillator and modulator are shown in the lower part of Fig. 2. The crystal tuning elements L_4 and C_3 were mounted near the crystal.

The following procedure was found useful in adjustment for the maximum diffraction effect. Before applying the rectangular wave modulation the amplitude of the crystal carrier oscillation was varied until the zero diffraction order was at its minimum intensity. For this adjustment the supersonic cell was placed so that the light beam passed close to the quartz crystal. The bar stop was next placed so as to intercept the zero order, and the photoelectric cell placed in the position of the eyepiece. The rectangular wave modulation was next applied and its amplitude varied until full modulation of the 8.5-megacycle carrier was obtained as shown by the oscillograph pattern, as in Fig. 3. This shows the envelope of the modulated carrier wave applied to the crystal. The amplitude of the pulses was next adjusted to the value obtained previously for minimum intensity in the zero order.

The oscillograph was used continuously to monitor the wave form applied to the quartz crystal. Inspection of this wave form gave the pulse ratio, i.e., the ratio of the duration of the pulse to the interval between corresponding points of succeeding pulses.

Only slight modifications of the arrangement of Fig. 2 were necessary when use was made of a moving focused spot on the screen. Inversion of the pulse applied to the cathode-ray tube grid, by the addition or removal of one stage of amplification, allowed its use as a blanking pulse to eliminate the return trace. A portion of the rectangular wave output applied as a synchronizing pulse at the sweep generator insured a constant phase relation between the lines on the screen and the wave pulses in the cell.

The High Speed Shutter

As a result of the adjustments described, the crystal is intermittently excited, producing groups or pulses of supersonic waves in accordance with the modulation. These short steep-sided pulses traverse the cell with high velocity and are absorbed by the glass wool at the opposite end of the cell. Each pulse in passing through the light beam diffracts the light so that it passes the opaque bar stop at S' and reaches the photoelectric cell. The speed of the shutter depends both on the repetition frequency of the rectangular wave and the ratio of this wave pulse to its cycle. For example, with a 20,000-cycle repetition frequency of the rectangular wave and with a pulse ratio of 20 percent the shutter speed, or open interval, is 10^{-5} second. Higher shutter speeds are readily obtained, either by decreasing the pulse ratio, or by increasing the repetition frequency with a given pulse ratio, or both.

Synchronization

Positive synchronization between the supersonic wave pulses and the periodic excitation of the phosphor was effected by controlling both from the same source. The excitation cycle, comprising the rise and decay of luminescence, was produced in two ways. In the first method tried the screen element of the cathode-ray tube was excited by a stationary unfocused electron beam which was modulated from cut-off to an intensity convenient for measurement of the emitted light. Synchronization between the wave pulses and the excitation cycle resulted from

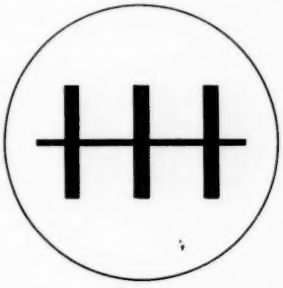

Fig. 3. Typical pattern shown by the monitoring oscillograph showing the envelope of the modulated 8.5-Mc carrier applied to the quartz crystal.

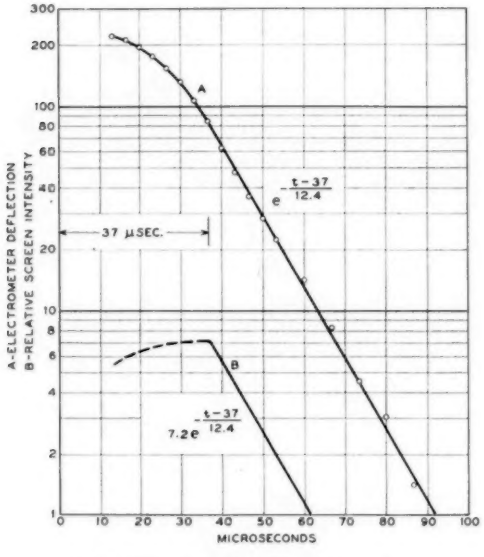

FIG. 4. Decay of $CdWO_4$. Stationary spot, 5-kc rectangular wave modulation.

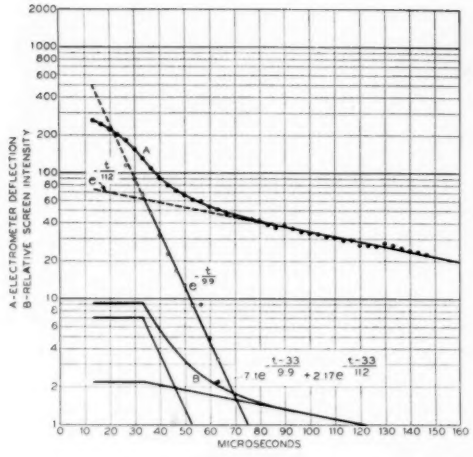

FIG. 5. Decay of ZnS–CdS. Stationary spot, 5-kc rectangular wave modulation.

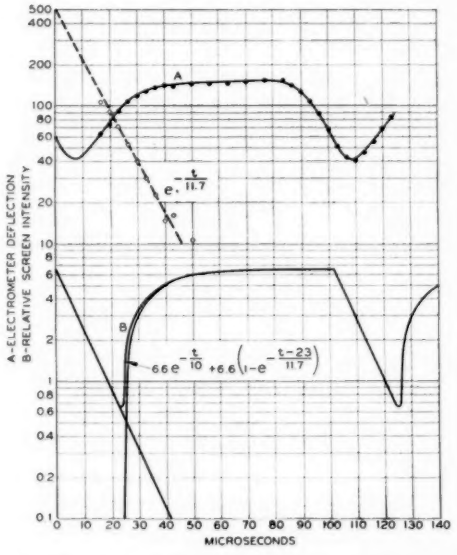

FIG. 6. Rise characteristic of $CaWO_4$. Stationary spot, 10-kc rectangular wave modulation.

feeding part of the rectangular pulse generator output as the modulating voltage to the cathode-ray tube grid and part to the modulator controlling the quartz crystal. With the light intensities required and the time necessary for a complete series of measurements the use of a stationary spot resulted in frequent burning of the screen. To avoid this a focused beam was made to scan a line or a raster with the return trace blanked out, and light from a short section of the scanned line was allowed to pass through the supersonic cell. In this case synchronization resulted from using a portion of the pulse generator output to control the line scan and the remainder as before to control the input to quartz crystal.

VARIABLE TIME DELAY

In order to measure the screen intensity at successive intervals during the rise and decay of luminescence it was necessary to provide for a variable time delay between the screen excitation and the arrival of the diffracting pulse at the section of the liquid traversed by the light beam. This was done by moving the supersonic cell by measured steps along its track so as to increase the distance between the quartz crystal and the light beam in the cell. Thus for a distance d in the liquid from the crystal, and a velocity V for the sound waves in water, the supersonic wave pulses lag by a time d/V with respect to the beam current pulses. For water $V=150{,}000$ cm/sec., so a 1-cm shift in position of the cell introduces an increase in time lag of 6.67×10^{-6} sec. The convenience and accuracy

of this means of controlling the time delay is apparent. The particular supersonic cell used in this work has a 22-cm clear aperture, allowing a maximum time delay of about 150 microseconds. This is ample for use with most high speed phosphors. For low speed phosphors measurements over a greatly extended time range are desirable. Such an extension was made by using a low frequency linear deflection of the electron beam and providing for successive shifts of the cathode-ray tube screen, the supersonic cell remaining stationary during the run. The collimator aperture was brought close to the screen so as to admit light from only a short section of the line. In a particular case a 60-cycle repetition frequency of the line scan was used. The length of the scanned line (blanking pulse removed) was 3.25 inches. Assuming 5 percent of the cycle was used for the return trace, the line was scanned in 15.8 milliseconds. From this the time scale along the line comes out $1'' = 4.87$ msec.

This latter method has several disadvantages: (1) The accuracy of the time scale is dependent on the linearity of the line scan, (2) different screen areas are used at each setting so that corrections are necessary to compensate for variations in screen efficiency due to imperfect screening, etc., and (3) the bulky cathode-ray tube is inconvenient to use as the moving element.

Corrections

At all cell settings a small, and for different positions of the supersonic cell a variable, amount of scattered light was encountered. This was corrected for by stopping the crystal oscillations and making a separate reading of the scattered light response. This was applied as a subtractive correction to the response with the crystal oscillator on.

Due to absorption of energy from the sound waves, the percentage of the incident light diffracted by a supersonic wave train decreases with increasing distance in the liquid. To correct for this, a factor for each cell position was obtained by substituting a constant intensity light source for the modulated light source.

Results

In the following section are shown some results obtained with the methods described in the preceding paragraphs. The data of Figs. 4, 5 and 6 were obtained with a stationary unfocused spot and a modulated cathode-ray beam. Those of Fig. 7 were obtained with a single line scan at 13-kc sweep frequency, the beam being well focused. The two long period curves of Fig. 8 were obtained with a 60-cycle line scan frequency. In these the cathode-ray tube was made

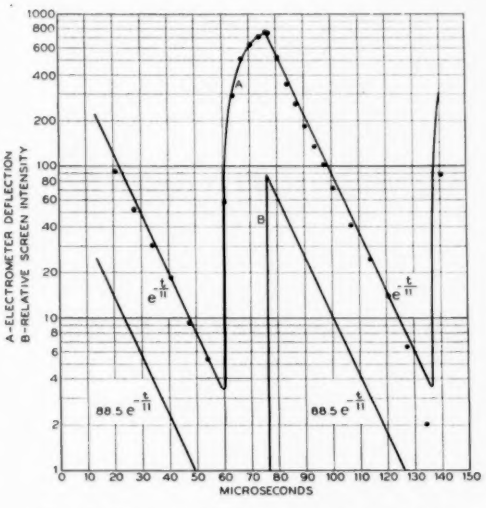

Fig. 7. Decay of $CdWO_4$. Moving focused spot.

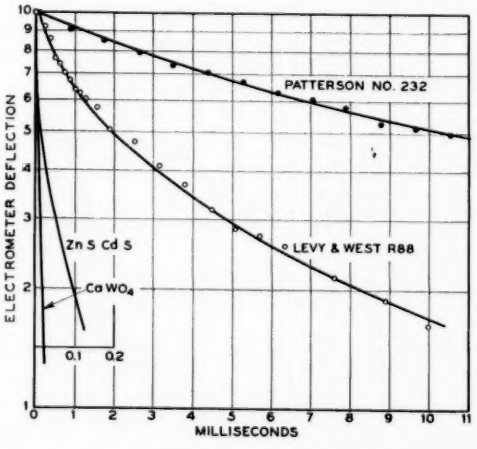

Fig. 8. Decay of two long lag phosphors. Insert shows two fast phosphors on a tenfold expanded time scale.

the movable element by mounting it on a lathe slide rest which had a calibrated screw motion.

From a consideration of the duration of the diffracting pulses, it follows that the screen intensity varies over a considerable range during the interval embraced by each diffracting pulse. The electrometer records the integrated response of the photoelectric cell to the light emitted during these time intervals. It is of interest to determine the relative screen intensities from the electrometer readings, or in other words, to apply an aperture correction to these readings. With these results, curves representing the relative screen intensities were built up. As a check, the electrometer response which would result from such an intensity distribution when scanned with the given aperture was calculated.

Figure 4 gives the measurement of the decay of $CdWO_4$ with a stationary spot, 5-kc rectangular wave modulation applied to the C.R.T. grid and the crystal oscillator, pulse ratio of *ca.* 18 percent.

The complete cycle of rise and decay has a period of 200 μsec. The exciting and diffracting wave pulses have equal durations of *ca.* 37 μsec. From $t=0$ to $t=37$ μsec. the diffracted light includes varying amounts of the rise characteristic. From 37 μsec. on the experimental points show the slope of the true decay response. From this slope the time constant of the decay is 12.4 μsec.

The aperture correction for the 37-μsec. diffracting pulse is easily made and the true screen intensities in terms of the electrometer response are obtained. For example, for $t=37$ μsec. the electrometer response is 84.2, hence

$$84.2=\int_{37}^{74} I_0 e^{-(t-37)/12.4}dt$$

from which $I_0=7.2$ and the expression for screen intensity is $I_t=7.2e^{-(t-37)/12.4}$. This is shown in the lower part of Fig. 4, along with the probable form of the rise curve as deduced from measurements to be described later (Fig. 6).

The full line curve shown passing through the experimental points was obtained by integrating the area under the intensity curves for successive 37-μsec. intervals.

Figure 5 gives the measurement of the decay of ZnS–CdS, with stationary spot, 5-kc modulation, and pulse ratio *ca.* 16 percent.

Analysis shows that, over the period of measurement, the decay may accurately be represented as the sum of two exponentials. The long period component of time constant 112 μsec. was obtained by inspection. Subtraction of the ordinates of this curve from the experimental points gave the open circled points shown. A straight line drawn through these points determined the time constant of the short period component as 9.9 μsec.

The initial intensities of the two components were obtained as before, giving as expressions of the screen intensity contributed by each component $I_t=7.1e^{-(t-33)/9.9}$ and $I_t'=2.17e^{-(t-33)/112}$. These two components and their sum are shown in the lower part of Fig. 5.

The full line curve shown passing through the experimental points was obtained by integration over successive 33-μsec. intervals of the area under the latter curve.

Figure 6 gives the measurement of the rise characteristic of $CaWO_4$, with stationary unfocused spot, 10-kc modulation, and pulse ratio for C.R.T. *ca.* 77 percent, for supersonic cell *ca.* 23 percent.

The preceding tests did not give satisfactory data from which to determine the form of the rise characteristic, as the diffracting pulse and the excitation interval were of the same duration. In order to make the conditions for studying the rise the same as were used for the decay, it was found convenient to invert the pulse applied to the cathode-ray tube grid. This gave a short decay interval followed by a comparatively long rise interval during which the screen element approached its maximum intensity. Inversion of the pulse was accomplished by adding one stage of amplification.

A trial was made with a $CaWO_4$ screen, using 10-kc modulation frequency. With the pulse ratios given, the duration of the supersonic wave pulse was 23 μsec., and the duration of screen excitation 77 μsec. The phase relation between the two pulses was such that the supersonic wave pulses started from the crystal at the instant the screen excitation stopped. The first measurements, starting with the light

beam near the crystal, gave points on the rise curve.

The variation of the screen intensity with time was obtained from the experimental points by first correcting each for the contribution due to the decay, the time constant of which had been obtained in a previous test. The resulting values were each subtracted from the maximum of 154, obtained from the experimental points, and gave the open circled points shown. These indicate an exponential rise of time constant 11.7 μsec. Intensities due to decay, rise, and their sum are shown in the lower diagram of Fig. 6.

Integration of the area under the latter curve for successive 23-μsec. intervals gave the full line curve shown passing through the experimentally determined points.

Figure 7 gives the measurement of the decay of $CdWO_4$, with single line scan of 13-kc repetition frequency, focused spot, oscillator output modulated at 13 kc, pulse ratio *ca.* 22 percent.

The use of the line scan is a convenient way for reducing the excitation time of a screen element, allowing higher screen intensities to be used without damaging the phosphor. In this test the collimator slit, which limits the screen element under test, was 1 mm. The transit time for the spot over this 1-mm element was *ca.* 1 μsec. Thus to a close approximation the particles of the screen element are subjected to simultaneous excitation.

The experimental points indicate an exponential decay of time constant 11 μsec. The expression for screen intensity obtained after making the aperture correction is $I_t = 88.5e^{-t/11}$. This is shown in Fig. 7, together with an assumed instantaneous rise. Integration of the area under this curve for successive 17-μsec. intervals gave the full line curve shown with the experimental values.

For a more detailed examination of the initial stages of decay a pulse generator giving a lower pulse ratio than that possible with the one used in this work would be desirable. Thus with a pulse ratio of 5 percent, the loss of light in the initial stages would not be serious and the shutter speed would be only 4 μsec.

Figure 8 gives measurement of the decay of two long lag phosphors, Patterson No. 232 and Levy and West No. R88 with a focused spot, raster scan, 60-cycle modulation and pulse ratio *ca.* 14 percent.

The results of measurements on the two long lag phosphors are included as an illustration of the use of an extended time range. Little work was done with this application of the method. With the Patterson sample separate readings of screen intensity were made at each setting which allowed a correction to be made for non-uniformity of the screen. This was not done with the R88 screen. No corrections for nonlinearity of scan were made in either case. The full line curves are drawn as an indication of the trend of the measured values. The decay curves for $CaWO_4$ and ZnS–CdS on an expanded time scale are included for comparison purposes.

Conclusion

The supersonic cell fluorometer is well adapted to investigations of the response of high speed phosphors. It allows measurements of the rise and decay of luminescence during time intervals much shorter than are practical with mechanical shutter arrangements. Shutter speeds are under easy and accurate control, with speeds of 1 μsec., or less, a distinct possibility. Positive synchronization between the shutter and the excitation cycle allows maximum utilization of the emitted light and makes possible the measurement of screen response directly in terms of photoelectric cell response. Finally, the device has the advantage of an accurately linear time base of such nature as to allow measurements of time of the order of 1 μsec. or less.

Acknowledgment is due to Mr. J. G. Knapp for assistance in assembling the apparatus and carrying out the measurements, and to Mr. F. R. Norton and Mr. J. R. Hefele for advice concerning the circuits used.

On the Phenomenon of "Fringes" in a Purely Corpuscular Theory of Light*

STEPHAN T. SERGHIESCO
Columbia University, New York, New York
(Received May 3, 1941)

IN this paper the analysis of the possibility of the formation of fringes by a group of lattices in a corpuscular theory of light, introduced through previous papers,[1] is continued. We shall discuss now the localized fringes produced by reflected and transmitted light and certain non-localized fringes whose measurements will lead to formulas similar to those of the Fresnel mirrors and Fresnel prisms experiments of the wave interference theory.

LOCALIZED FRINGES

The fringes studied before, which were produced by reflected light in a film of lattices and whose measurements led us to a similar formula of the stationary waves phenomenon or of Newton's rings phenomenon, were of this type. They represent the variation in the intensity of light which is obtained by summing up the intensities of all the rays passing through each point of the boundary of the film; as these rays diverge themselves as soon as they pass through these points these localized fringes are produced right on the boundary itself and they appear as if they were painted on the film.

Localized fringes can also be produced by transmitted light; nevertheless they appear less noticeable due to the decrease in the intensities of the rays producing them and also to the fact that the whole phenomenon is produced in an illuminated field. Before proceeding further with the study of these fringes, let us mention here a detail in the variation of the intensity of light on a face of a dihedral angle. In the general method exposed before, the dihedral angle has been considered as an independent unit; let us take now the combination of two of these dihedral angles and see what changes will occur in the shape of the curve of the intensity of light on the boundary of one of them only. In Fig. 1, the light is supposed to fall from above OA. The intensity at a point m of OA will be equal to the sum of the intensities of all the rays passing through m. Or, all the rays falling on these dihedrals can be divided into groups forming two kinds of beams; beams composed of rays reflecting between OA and OB and beams composed of rays reflecting between BO and BO'. The graph of the intensity of light on the upper boundary will have two important maxima in A and O, and since, following the points of the boundary, there is an unbalanced energy in the points A and O due to the asymmetry in the arrangement of the dihedral angles with respect to these points, it is to be expected that these maxima will be unequal. If we have a combination of several dihedrals, we will encounter a greater complexity of rays; nevertheless, the study of the intensity of light on the boundary OA can be drawn, in a first approximation, by considering the vertices of all these dihedral angles as separate luminous centers.

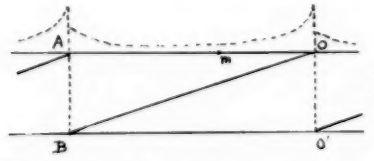

FIG. 1.

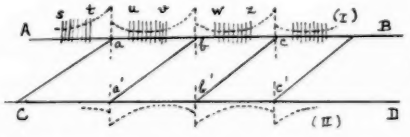

FIG. 2.

Let us now return to our localized fringes produced by reflected and transmitted light. If we consider a film of lattices (Fig. 2) bounded by two parallel corpuscular planes AB and CD including, for the sake of simplicity, only one layer of cells, let us assume that the vertices a; a' and b; b' are on lines parallel to the line of vision. When the eye and the source of light are on the same side of the film (above AB) the curve (I) would be the graph of the intensity

* Publication assisted by the Ernest Kempton Adams Fund for Physical Research of Columbia University.
[1] S. Serghiesco, Comptes rendus **202**, 1563, 1761, (1936); J. Opt. Soc. Am. **31**, 109 (1941).

of localized fringes by reflection, and when the eye is opposite the source of light with respect to the film, the curve (*II*) will represent the graph of the intensity of the localized fringes produced by transmission. Let us now divide the space *AB* into different regions of bright and dark fringes *tu*; *uv*; *vw*; ···. When we pass from reflected to transmitted light no definite law can be drawn in general about the transformation of these two kinds of fringes, the result depending on the nature of lattices, angle of incidence and the line of vision. Nevertheless, in the case described above, one can see that if the line of vision is kept the same, while the line of highest brilliancy in the bright fringes will keep more or less the same position, the right and left neighboring lines will reverse their intensities when passing from reflected to transmitted light (the curve (*II*) being abrupt to the left and less abrupt to the right at the points *a'*; *b'*; *c'*; ··· due to the position of the dihedral angles in the lower layer). We will discover, therefore, in this case, only a shift or a displacement of fringes, rather than a total transformation of bright fringes into dark fringes, or vice versa (which was the only case of transformation possible in the wave theory).

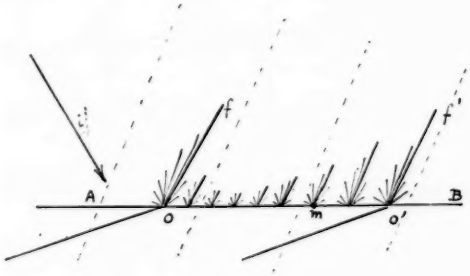

FIG. 3.

NON-LOCALIZED FRINGES PRODUCED BY GROUPS OF LATTICES

Let us consider again a film of lattices bounded by parallel corpuscular planes upon which is falling a beam of homogeneous light of incidence *i* (Fig. 3). The light produced in the space above *AB* will be composed of the rays reflected directly by the plane *AB* under an angle equal to the angle of incidence and also of the rays which penetrate beyond *AB* and are then reflected back

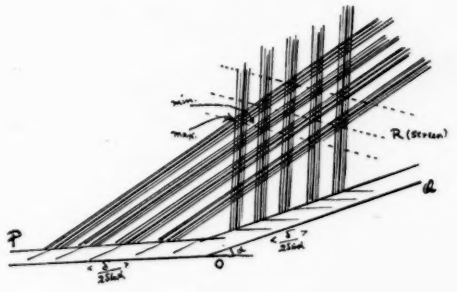

FIG. 4.

into this space. Through every point *m* of the boundary *AB* there will be a multitude of rays coming from the interior of the film and diverging in all directions from 0° to 180°, because the dihedral angles, forming the first layer under the boundary line, will be subjected to beams of light of different directions coming from beneath. From the study of the dihedral angle, one can learn that the intensity of the rays passing through the fixed point *m* varies with the direction of the ray, increasing when this direction approaches the position which makes an angle with *AB* equal to the angle of incidence; we also learn that the intensity of every one of these rays is increasing when the point *m* is approaching the points of the boundary corresponding to the vertices of the different dihedral angles. If we represent these different rays by vectors whose lengths designate their respective intensities, the distribution of the rays and their intensities in the space immediately above *AB* will appear, therefore, as in Fig. 3, which represents a section perpendicular to the edges of the different dihedral angles. The points will appear, then, more or less as luminous centers sending their maximum of intensity in the directions *of*; *of'*; *of''*; ··· which make with the boundary an angle equal to the angle of incidence, such that on a screen perpendicular to this direction there will be periodic maxima and minima. The space above *AB* could then be divided into regions of different intensities. The difference between the intensities of these regions is not great enough to make them really noticeable at an appreciable distance from the boundary; that is why one must always analyze them near the group of lattices considered.

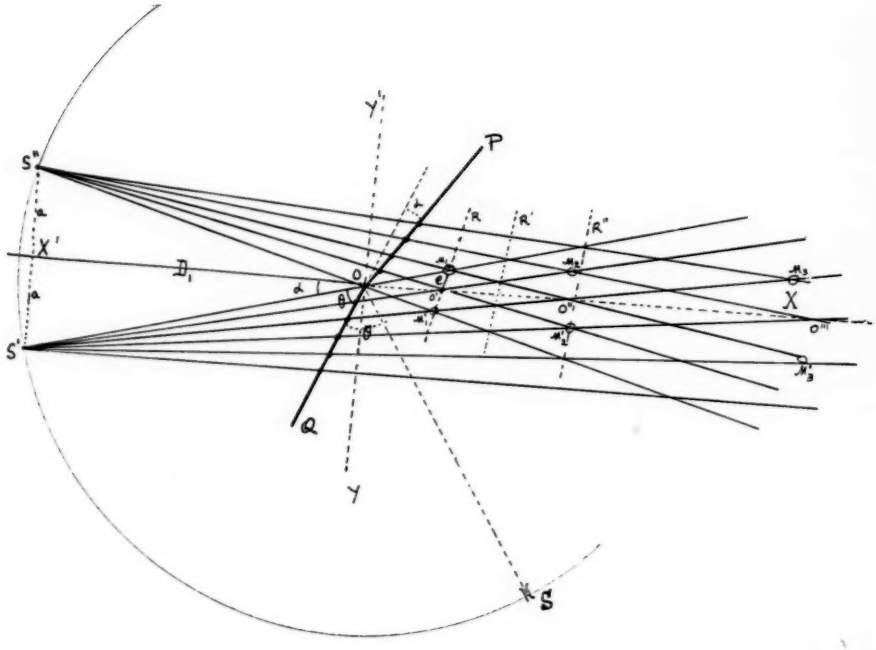

FIG. 5.

If the same homogeneous beam of light will fall on another identical film of lattices or on a prolongation of the same group of lattices as in Fig. 4 the second group of lattices will produce also a series of regions of different intensities, and the intersections of these two series of regions will give out bands of greater differences of intensities and, therefore, more noticeable dark and bright bands. For instance, where two regions of higher intensities meet there will be a maximum, and where two regions of lower intensities meet there will be a minimum. As this figure represents a section perpendicular to the planes P and Q of the two groups of lattices, the resulting bands of maxima and minima will therefore be perpendicular to the plane of this section—that is to say to the plane of the figure. The distance between two consecutive initial regions coming out of the films P and Q is $\delta/2 \sin \alpha$, the distance between the parallel equidistant planes of the film of the two lattices being $\delta/2$.

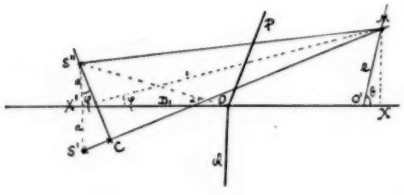

FIG. 6.

ON THE MEASUREMENTS OF NON-LOCALIZED FRINGES PRODUCED BY LATTICES

Let S represent in Fig. 5 a source of homogeneous light (for instance, a slit parallel to the planes of the lattices P and Q). Let θ represent the angle SOQ, and S' and S'' the two virtual

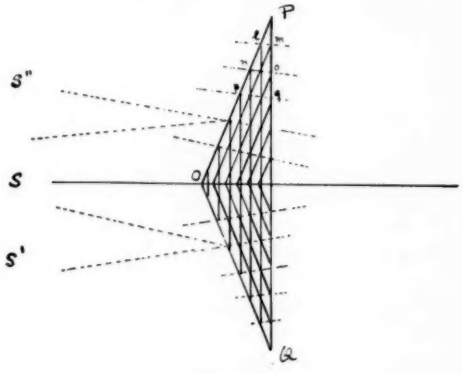

FIG. 7.

FIG. 8.

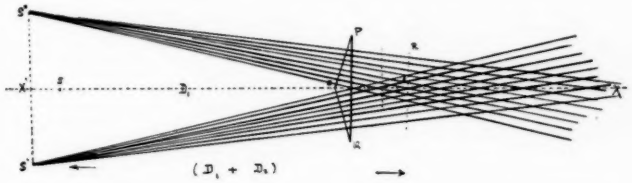

sources with respect to the planes P and Q. The distances from the special fringes under consideration to the films of lattices and to the source of light are, respectively, D_2 and (D_1+D_2). As the angle α made by the two groups of lattices is supposed to be extremely small, the chord $S'S''$ is also very small. In our figure the angle α, and therefore the segment $S'S''$, has been exaggerated in order to obtain the intersection of the two beams of light toward the center of the figure. If two perpendicular lines $X'X$ and $Y'Y$, having their point of intersection in O, are taken as axes ($X'X$ being also perpendicular to $S'S''$), the coordinates of the different points on the films P and Q marking the distance between two consecutive initial regions will be, respectively:

$$x=\frac{\delta}{2\sin\alpha}\cos\theta, \quad y=\frac{\delta}{2\sin\alpha}\sin\theta$$

and

$$x'=-\frac{\delta}{2\sin\alpha}\cos(\theta+\alpha), \quad y'=-\frac{\delta}{2\sin\alpha}\sin(\theta+\alpha)$$

δ and α being very small, it can be shown that a line passing through any two points like $O'M_1$; $O'M'_1$; M_1M_1'; $\cdots$ (corresponding, for instance, to bright fringes) makes, approximately, an angle θ with $X'X$ (if we neglect powers of δ and also α in trigonometric functions of $(\theta+\alpha)$). The distance e between two bright fringes on a certain position of the screen R can then be obtained from any triangle whose base is e and vertex S' or S''. Either triangle being divided by P or Q into two similar triangles we have:

$$e=\frac{\delta}{2D_1\sin\alpha}\cdot(D_1+D_2)=\frac{\delta}{2\alpha D_1}\cdot(D_1+D_2),$$

which becomes *Fresnel-mirrors measurement formula* if we replace δ by λ.

Under a normal incidence (θ almost 90°) the points of intersection of initial regions O', O'', O''', $\cdots$ are very near $X'X$ which can be taken as their line of regression. It can then be shown that points like M_1; M_2; M_3; $\cdots$ (representing the feet of a fringe of a certain order in the plane of the figure when the screen R moves parallel to it) are on a *hyperbola* of foci S' and S''. In Fig. 6 let $2a$ represent the distance $S'S''$ of the two virtual sources of light, and let us draw from M as center with MS'' as radius an arc $S''C$. Since $S'S''$ is extremely small and $X'O$ very great, the arc $S''C$ can be considered as a straight line perpendicular to MS' and therefore the angle φ equal to the extremely small angle $MX'X$. The difference between MS' and MS'' is: $S'C=2a\sin\varphi=2a\varphi$ or from triangle $MX'X$:

$$\tan\varphi=\varphi=\frac{MX}{X'X}=\frac{e\sin\theta}{D_1+D_2}=\frac{\delta\sin\theta}{2\alpha D_1}=\frac{\delta\sin\theta}{2a}$$

therefore $S'C$ is constant and equal to

$$2\cdot\delta/2\cdot\sin\theta.$$

When the groups of lattices form a biprism of very small angle (Fig. 7) where one series of equidistant corpuscular planes are parallel to PQ and another series parallel to OP and OQ respectively, the lines lm, no, pq, $\cdots$ of the vertices of the different cells are perpendicular to bisectors at P and Q and correspond to regions of greatest intensities. Since the angle α is very small we may consider the light from a source S to be passing through the prism at minimum deviation and therefore in a direction parallel to these lines. The distances are almost equal to half of the diagonal of a cell—that is, to $d/2\sin\alpha/2$ where d is the common distance between the parallel planes forming the lattices. The distance e between two bright or dark fringes on a screen (Fig. 8) will then be:

$$e=\frac{d}{2\sin\alpha/2}\frac{(D_1+D_2)}{D_1}=\frac{d}{\alpha}\frac{(D_1+D_2)}{D_1}.$$

If n is the index of refraction of the medium in which these lattices are imbedded, it will be sufficient to take the distance d equal to $\delta/2(n-1)$ (differing from its optical equivalent by $\delta/2$ of the preceding combinations of lattices), in order to arrive to the same measurement formula with the *Fresnel-biprism formula* of the wave interference theory.

Under the boundary of a biprism there are other combinations of lattices possible; they would lead to other fringes and therefore to other measurement formulas.

AUGUST, 1941 J. O. S. A. VOLUME 31

Angular Distribution of Light Scattered in Liquids

L. H. DAWSON AND E. O. HULBURT
Naval Research Laboratory, Washington, D. C.

(Received May 31, 1941)

With a Macbeth illuminometer and a Nicol prism, measurements were made of the intensities of the polarized components of the light from a tungsten lamp scattered at angles from 22½ to 157½ degrees in ethyl ether, carbon tetrachloride, carbon disulphide, benzene and water. All of the liquids were fairly, but not completely, free of optical impurities. The observations were found to agree with the theory that the scattering centers in the liquids scattered in the manner of particles small with respect to the wave-length with an additional scattering independent of direction and state of polarization, the amount of the additional scattering depending on the liquid. Deviations from the theory were such as would be accounted for by the optical impurities. For water, strong forward scattering was observed, obviously due to the visible motes.

INTRODUCTION

PREVIOUS investigations of the scattering of light in liquids have been mainly concerned with the light scattered at right angles to the direction of the incident beam, with its state of polarization, and with the variation of the intensity of the right angle scattered light with wave-length and with the chemical and physical properties of the liquid. The angular distribution of the light scattered in pure liquids has not been observed. The intensity of the light scattered at several angles by a sample of sea water was measured[1] and considerable forward scattering was observed which was attributed to optical impurities in the water. In the present experiments the scattering at various angles was observed for five liquids, ethyl ether, carbon tetrachloride, carbon disulphide, benzene and water, the liquids being selected to cover a wide range of optical properties. The measurements were found to be in approximate agreement with a simple theory.

[1] K. R. Ramanathan, Phil. Mag. **46**, 543–553 (1923).

THEORETICAL

Let i_0 be the intensity of a beam of unpolarized light passing through a liquid and i' the intensity of the light scattered at right angles to i_0 per unit solid angle per unit volume of the liquid. The density fluctuation theory of Einstein[2] and Smoluchowski[3] states that

$$i' = i_0 \frac{\pi^2}{18} \frac{\eta k T}{\lambda^4} (\mu^2-1)^2(\mu^2+2)^2, \qquad (1)$$

where λ is the wave-length of light, μ the refractive index of the liquid, η its isothermal compressibility, T the absolute temperature and k the Boltzmann constant 1.372×10^{-16} erg deg.$^{-1}$. According to the theory the scattering centers were small with respect to λ and isotropic. For gases (1) reduces to the Rayleigh equation. (1) was found to be in approximate, but not exact, agreement with observations on various gases and liquids, the calculated values being

[2] A. Einstein, Ann. d. Physik **33**, 1275–1298 (1910).
[3] M. v. Smoluchowski, Ann. d. Physik **25**, 205–226 (1908).

below the observed values.[4, 5] The variation of i' with λ given by (1) was observed[6] to be true within the error of experiment for water throughout the wave-length interval from 5790 to 2536A.

Let ϕ be the angle between the directions of the incident and the scattered light. Let i be the total intensity of the light scattered at angle ϕ, and i_v and i_h its polarized components, i_v being the component with electric vector normal to the incident beam. If the incident and scattered beams are in the horizontal plane, the electric vectors of i_v and i_h are vertical and horizontal, respectively. Let i', i'_v and i'_h be the respective values of i, i_v and i_h for $\phi=\pi/2$. Then

$$i=i_v+i_h \quad \text{and} \quad i'=i'_v+i'_h. \tag{2}$$

Define δ by

$$\delta=i'_h/i'_v. \tag{3}$$

According to elementary theory for isotropic scattering centers of dimensions small with respect to λ

$$i_v=i'_v=a^2 \quad \text{and} \quad i_h=a^2\cos^2\phi, \tag{4}$$

where a^2 is a constant. Then

$$i=i'(1+\cos^2\phi). \tag{5}$$

From (3) and (4) $i'_h=\delta=0$ and the light i' scattered at $\phi=\pi/2$ is completely polarized.

It was observed,[5, 7] however, that i' was never completely polarized in the cases of all substances yet examined. Thus δ was not zero; δ was termed the "polarization defect." On the assumption that the scattering centers were anisotropic a modifying term for (1) was worked out by Cabannes which resulted in multiplying the right-hand side of (1) by

$$6(1+\delta)/(6-7\delta). \tag{6}$$

From the nature of the calculation (6) did not apply for δ greater than 0.5. One theory[8] connected δ with the anisotropy of the molecules in the gaseous condition and another theory[9] with the electric double refraction of the liquid. Comparison with observation[10] showed that (1) multiplied by (6) gave agreement within about 2 percent for δ less than 0.1, but for liquids for which δ was above 0.3 the theoretical values of i' were greater than the observed values, being in many, but not all, cases about 15, 25 and 80 percent greater for $\delta=0.3$, 0.5 and 0.6, respectively. It appeared that the correction term (6) was unsatisfactory for δ greater than about 0.2.

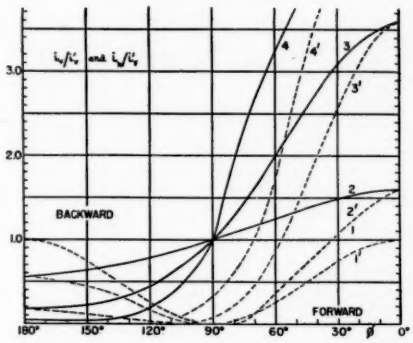

FIG. 1. Unprimed and primed curves, theoretical values of i_v/i'_v and i_h/i'_v for particles of various sizes. Curves 1 and 1', radius small with respect to λ; curves 2 and 2', 3 and 3', and 4 and 4', respectively, radius equal to $\lambda/6.67$, $\lambda/4.28$ and $\lambda/3.59$.

It was observed[11] that the scattered light at $\phi=\pi/2$ was unpolarized when the incident light was polarized with electric vector parallel to the plane containing the incident and scattered beams. This indicated that the scattered light might be accounted for by assuming that anisotropy of the scattering centers was such that in addition to the intensity given by (4) they scatter an unpolarized intensity $2b^2$ equally in all directions. Then

$$i_v=i'_v=a^2+b^2, \tag{7}$$

$$i_h=a^2\cos^2\phi+b^2, \tag{8}$$

and

$$\delta=b^2/(a^2+b^2). \tag{9}$$

For the purpose of comparison with experiment it is convenient to derive from (2), (7), (8) and (9) the relations

$$i_v/i'_v=1, \tag{10}$$

[4] J. Cabannes, Ann. d. Physik **15**, 1–149 (1921).
[5] C. V. Raman, *Molecular Diffraction of Light* (University of Calcutta Press, 1922).
[6] L. H. Dawson and E. O. Hulburt, J. Opt. Soc. Am. **27**, 199–201 (1937).
[7] W. H. Martin and S. Lehrman, J. Phys. Chem. **26**, 75–88 (1922).
[8] C. V. Raman and K. R. Ramanathan, Phil. Mag. **45**, 113–128 (1923); C. V. Raman and K. S. Rao, Phil. Mag. **45**, 625–640 (1923).
[9] R. Gans, Zeits. f. Physik **17**, 353–397 (1923).
[10] K. S. Krishnan, Phil. Mag. **50**, 697–715 (1925).
[11] Reference 5, page 57.

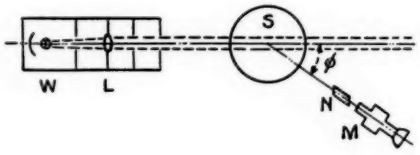

FIG. 2. Light scattering apparatus.

and

$$i_h/i'_v = \delta + (1-\delta)\cos^2\phi. \tag{11}$$

Further, one obtains

$$i = i'\left(1+\frac{1-\delta}{1+\delta}\cos^2\phi\right). \tag{12}$$

The complete expression for the scattered intensity is, from (1), (6) and (12),

$$i = i_0\frac{\pi^2}{18}\frac{\eta kT}{\lambda^4}(\mu^2-1)^2(\mu^2+2)^2\frac{6(1+\delta)}{6-7\delta} \times\left[1+\frac{1-\delta}{1+\delta}\cos^2\phi\right]. \tag{13}$$

In Fig. 1, curve 1 from (10) and curve 1′ from (11) with $\delta=0$ show that the scattering is symmetrical on either side of $\phi=\pi/2$ and is equal backward and forward; this is also true for $\delta\neq 0$. The other curves of Fig. 1 bring out the manner in which particles of dimensions comparable with the wave-length λ influence the scattering. Curves 2 and 2′, 3 and 3′, and 4 and 4′, for i_v/i'_v and i_h/i'_v, respectively, refer respectively to spheres of radii equal to $\lambda/6.67$, $\lambda/4.28$ and $\lambda/3.59$. It is seen that the forward scattering for each polarized component increases with the radius of the sphere. The data of the curves are from calculations by Rayleigh[12] for transparent spheres of refractive index 1.5. In Rayleigh's notation $i_v/i'_v = [\text{modulus } Y]^2$ and $i_h/i'_v = [\text{modulus } (yZ-zY)]^2$.

EXPERIMENTS AND RESULTS

In the first experiments the scattering chamber containing the liquid was a Pyrex glass spherical flask 17 cm in diameter with nine short side tubes sealed to it, placed every $22\frac{1}{2}$ degrees from $\phi=0$ to 2π; the tubes were closed with quartz plates. Except for the quartz windows the entire outside of the chamber was painted black. With a high pressure mercury arc and a Geiger photo-tube with appropriate counting circuit measurements of i/i' were made for the 366 line of mercury. With a 1000-watt tungsten lamp, blue, yellow and red filters and a Macbeth illuminometer measurements of i/i' were made for the blue, yellow and red regions of the spectrum. Observations on water, benzene and carbon tetrachloride showed that the i/i', ϕ curves were the same for the various spectral regions within the error of experiment which was about 5 and 10 percent for the visual and ultraviolet measurements, respectively. With the establishment of this fact there appeared little to be learned by extending the measurements to other liquids, and attention turned to measuring the polarized components. From general considerations some dispersion of the i/i', ϕ curves might be expected, but if dispersion exists greater accuracy than 5 percent is needed to bring it out.

Spherical Pyrex glass flasks 17 cm in diameter were used as scattering chambers. These were more satisfactory than the flask with nine side tubes, being relatively easy to clean. They were left unpainted to permit inspection of the liquid from every point of view, for it soon became apparent that the major difficulties were not in the photometric measurements, which were rela-

TABLE I. *Values of polarization defect δ.*

	MARTIN AND LEHRMAN[a]	RAMAN AND RAO[b]	KRISHNAN[c]	DAWSON AND HULBURT
Ether	0.10	0.083	0.089	0.10
CCl_4	—	0.110	0.061	0.076
CS_2	0.71	0.700	0.70	0.63
C_6H_6	0.48	0.398	0.48	0.47
Water	0.067	0.125	0.96	0.10

[a] See reference 7 in text.
[b] See reference 8 in text.
[c] See reference 10 in text.

TABLE II. *Values of i′ relative to ethyl ether.*

	MARTIN AND LEHRMAN[a]	RAMAN AND RAO[b]	KRISHNAN[c]	DAWSON AND HULBURT
Ether	1.00	1.00	1.00	1.00
CCl_4	—	1.21	1.02	0.97
CS_2	12.8	18.6	13	10.9
C_6H_6	2.82	3.60	3.15	2.70
Water	0.19	0.19	0.21	0.19

[a] See reference 7 in text.
[b] See reference 8 in text.
[c] See reference 10 in text.

[12] Rayleigh, Proc. Roy. Soc. **A84**, 25–46 (1911).

FIG. 3.

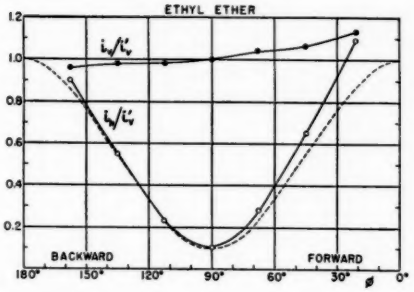

FIG. 4.

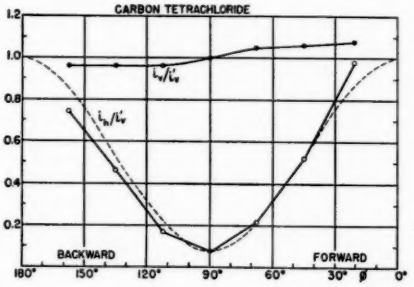

FIG. 5.

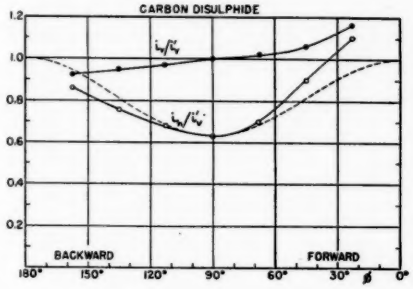

FIG. 6.

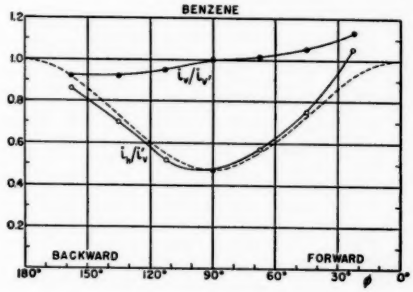

FIG. 7.

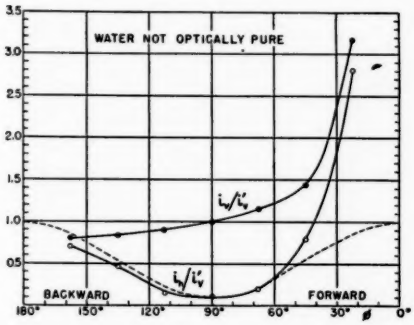

FIGS. 3 to 7. Dots and circles, observed values of i_v/i'_v and i_h/i'_v; dotted curves, theoretical values of i_h/i'_v from (11).

tively simple, but in obtaining and keeping the liquids free from optical impurities. Figure 2 gives a plan view of the optical apparatus. The light from a 1000-watt tungsten lamp W in a black housing with diaphragms was focused into a beam by lens L. By adjustment of the lens the beam was made slightly diverging so that it was parallel, and about 15 mm in diameter, in its passage through the scattering chamber S. The scattered light was viewed at angle ϕ through the Macbeth illuminometer M and Nicol prism N. M and N were on a movable arm and could be swung to various angles ϕ; N could be rotated on its axis. A pale blue filter was placed over the comparison lamp of the illuminometer to give a fair color match with the scattered light. There were a few reflections from the walls of S which were avoided. All observations were made at room temperature about 20°C.

Five liquids were measured, ethyl ether, carbon tetrachloride, carbon disulphide, benzene and water. These were chemically pure and were freed as much as possible from optical impurities by slow distillation in quartz when necessary and by allowing to stand in their flasks for weeks. An extremely sensitive test was to examine the beam of light in the flask of liquid with a low power microscope at small angles of ϕ. Motes and particles which were invisible at $\phi > 40°$ became very visible at $\phi < 20°$. Such a test could not, of course, insure that all dust or motes were absent, for very small motes might still escape detection, and in the end one can probably never be entirely certain that all optical impurities are removed and that the measurements refer to a pure liquid. None of the liquids was brought to a condition where no motes could be seen at small values of ϕ, but no motes were visible at $\phi = \pi/2$. Except in the case of water it was judged that the motes were few and added little to the light scattered

TABLE III. *Polarized components of the scattered light.*

ϕ	ETHER		CCl_4		CS_2		C_6H_6		WATER	
	i_v/i'_v	i_h/i'_v	i_v/i'_v	i_h/i'_v	i_v/i'_v	i_h/i'_v	i_v/i'_v	i_h/i'_v	i_v/i'_v	i_h/i'_v
$22\frac{1}{2}°$	1.13	1.09	1.08	0.98	1.16	1.10	1.13	1.05	3.16	2.80
45°	1.06	0.65	1.06	0.52	1.06	0.90	1.05	0.75	1.43	0.78
$67\frac{1}{2}°$	1.04	0.28	1.05	0.22	1.02	0.70	1.01	0.57	1.15	0.21
90°	1.00	0.10	1.00	0.076	1.00	0.63	1.00	0.47	1.00	0.10
$112\frac{1}{2}°$	0.98	0.23	0.96	0.17	0.97	0.68	0.95	0.52	0.92	0.15
135°	0.98	0.55	0.96	0.46	0.95	0.76	0.92	0.70	0.83	0.46
$157\frac{1}{2}°$	0.96	0.90	0.96	0.74	0.92	0.86	0.92	0.86	0.80	0.69

by the main body of the liquid. Water is discussed in more detail later.

In Tables I and II are given the values of δ and i' obtained by various observers, the fourth column of Table II being obtained with the apparatus of Fig. 2 with the Nicol prism removed. The values of i' of Table II are relative to ethyl ether, since the liquid is readily prepared of high optical purity and has been used as a standard by others. It is seen that the present values of δ and i' are about as low as those of others. Since optical impurities may be expected to increase i' and usually, but not necessarily, to increase δ, the comparison shows that as far as these quantities are concerned the liquids of the present measurements were about as dust free as those of others. The optical properties of the liquids covered a considerable range, for as seen from the tables the light scattering power varied by a factor of 50, being lowest for water and highest for carbon disulphide, and the polarization defect varied from 0.076 for carbon tetrachloride to 0.63 for carbon disulphide.

The observed values of i_v/i'_v and i_h/i'_v are in Table III, and are plotted as ordinates in the dots and circles, respectively, of Figs. 3–7. The straight lines $i_v/i'_v=1$ parallel to the ϕ axis are the theoretical curves of (10) and the dotted curves are the theoretical values of i_h/i'_v calculated from (11) with the observed values of δ from Table I. It is seen that the observed and theoretical curves of all the liquids except water are in fair agreement. There is a slight upward tilt of the observed curves relative to the theoretical curves which may be due to optical impurities. The agreement of observation and theory indicates that the scattering centers in the liquids scattered in the manner of particles small with respect to the wave-length with an additional scattering which was independent of direction and state of polarization, the amount of the additional scattering depending on the liquid.

Water is notoriously difficult to prepare dust free,[13] and since the scattering power of water is very low the influence of optical impurities is important. When distilled very slowly in quartz and collected in Pyrex, the water contained a considerable quantity of motes which did not disappear with standing for weeks. Rinsing and repeating the distillation made no improvement. The motes were barely visible at $\phi=\pi/2$, but were readily seen at $\phi<20°$ appearing as bright sparkles of light which moved and changed suddenly and erratically as by Brownian motion. One had the impression that they were pieces of glass. The curves of Fig. 7 refer to the purest water collected in Pyrex from the quartz still; the water contained many motes visible at $\phi<20°$ and the forward scattering evidenced by the curves was obviously due to the motes. Purer water was obtained by collecting in a quartz vessel. But no large spherical quartz flask suitable for the scattering measurements was at hand and the investigation was brought to an end.

[13] Reference 5, page 46.